

Thursday Posters

Fidelity of near resonant states in the kicked rotor

P. D. McDowall, A. Hilliard, M. McGovern, T. Grünzweig, M. F. Andersen

Jack Dodd Centre for Quantum Technology, Department of Physics, University of Otago, New Zealand

We investigate the dynamics of the atom-optics δ -kicked rotor in the vicinity of quantum resonance^{1,2}. Although small deviations from resonant conditions lead to a negligible change in the momentum space probability density, they lead to a significant relative phase change between the different momentum states taking part in the dynamics. By adding a strong, phase-inverted pulse to the kicked rotor pulse sequence, one can measure the overlap between the resonant state and any other state, i.e., perform a fidelity measurement. Such a measurement is sensitive to the relative phase changes of the different momentum states as well as changes in the momentum space probability density.

When the initial state is a plane wave, the proposed sequence shows a resonant peak of height one in the fidelity measurement when the time between pulses, T , is scanned across the Talbot time. The width of this peak is narrower than the peak observed in the energy transferred to the atoms around resonance (see Fig. 1). The width of the fidelity peak scales as $1/N^3$, where N is the total number of pulses in the sequence, whereas the energy peak scales as $1/N^2$. This reveals that important information (in this case, relative phase between momentum components) of near resonant states is not captured by investigations of the transferred energy. We also consider a Gaussian wavepacket as our initial state and find that for a low number of pulses, the Gaussian wavepacket returns a narrower fidelity peak than both the plane wave case and the energy peak around quantum resonance, whereas the opposite is true for large N . This narrow fidelity peak provides a method for accurately measuring the Talbot time that, together with other well known constants, constitutes a measurement of the fine structure constant³.

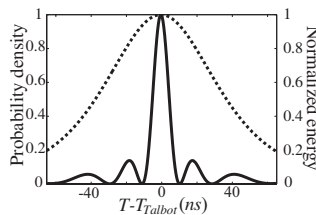


Figure 1: *Dashed line: Energy of atoms initially in $|p = 0\rangle$ after an experimentally realisable pulse sequence normalized to the on-resonance energy, as a function of the time between pulses T for ^{85}Rb ; Solid line: Numerical evaluation of the proposed fidelity measurement. Both peaks are centred around the Talbot time $T = T_{\text{Talbot}} = 64.8 \mu\text{s}$.*

¹M. G. Raizen 1999 *Adv. At. Mol. Opt. Phys.* **41** 43

²W. H. Oskay, D. A. Steck, V. Milner, B. G. Klappauf and M. G. Raizen 2000 *Opt. Commun.* **179** 137

³P. McDowall, A. Hilliard, M. McGovern, T. Grünzweig and M. F. Andersen 2009 *New J. Phys.* **11** 123021

Nondispersivity of the scalar Aharonov-Bohm phase observed in the Ramsey atom interferometry with a cold atomic ensemble

Atsuo Morinaga, K. Numazaki and H. Imai

Tokyo University of Science, Noda-shi, Chiba, Japan

The scalar Aharonov-Bohm phase is realized if particles move in a force-free space; that is, the time-dependent potential must be uniform in the interrogation space. We demonstrated this situation over 1000 fringes using a cold ensemble of sodium atoms of $m=0$ spin states released from a magneto-optical trap in a time-dependent magnetic field.

In order to make an atom interferometer, two two-photon stimulated Raman pulses (Fig. 1) were applied to atoms with an interrogation time of 5 ms, where the wave function is described as the tensor product of the external motional states and the internal states:

$$\Psi = \Phi(x, t) \otimes \chi = \sum_n e^{ik_n x - \omega_n t + \phi_n} (|F=1\rangle e^{i\delta_1} + |F=2\rangle e^{i\delta_2})$$

Then the phase in the external part depends on velocity dispersion in spatial inhomogeneity of potential. The calculation of the magnetic field showed a gradient of 10 % of the field strength in 4 mm, where the cold sodium atoms move on average during two pulses. This variation changes the second-order Zeeman energy by 20 %, but it is only 10^{-4} of the kinetic energy of cold sodium atoms at a temperature of 200 μK . Then the velocity of atoms changes only by a ratio of 10^{-4} . We measured the population probability at a resonance frequency as a function of the magnetic field strength, as shown in Fig. 2¹. We can see the 18 fringes with almost the same amplitude. The population probability was fitted with the cosine curve whose amplitude decreases at a time constant of $2.5 \pm 7.8 \text{ mT}^2$.

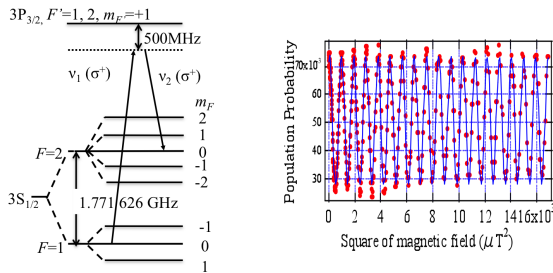


Figure 1: *Simulated Raman transition*

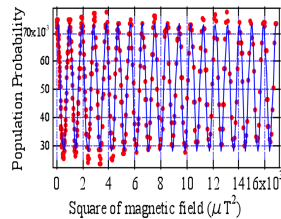


Figure 2: *Interference fringes due to SAB effect*

¹K. Numazaki et al., Phys. Rev. A 81, 032124 (2010).

An atom interferometer on a chip

V.A. Prieto^{*1}, J. Alexander^{*1}, C. Rowlett^{*}, W.M. Golding^{*}, P.J. Lee^{*}

^{*}*Sensors and Electron Devices Directorate, US Army Research Lab, Adelphi, MD*

We report on recent experimental progress towards developing a compact atom interferometer on an atom chip. The interferometer uses ⁸⁷Rb atoms magnetically confined in an atomic waveguide produced by wires on the surface of a lithographically patterned chip. We study various current configurations in our chip wires. Figure 1 shows the type of current density distortion that can occur at simple wire junctions. Distortions like these cause significant deviations of the local magnetic potential and are caused by the modified boundary conditions on current flow that occur at the wire junction. Interesting new trap and interferometer designs based on control over the local current density at wire junctions are currently being studied using numerical techniques.

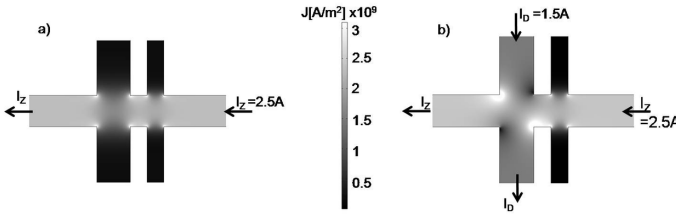


Figure 1: *Current Density Distribution in a) the Z wire and b) the Dimple wire configurations for the given currents.*

We study the combination of different current configurations with various external bias fields that can offer the means to create well-controlled and repeatable coherent splitting of the atomic cloud through dynamically adjusting the currents and bias fields. Figure 2 shows the magnetic field for a fixed current configuration on our chip and various bias fields. We also investigate dynamic transformations between different double-well configurations with the atoms in-situ and observe the effects on the initially trapped atoms.

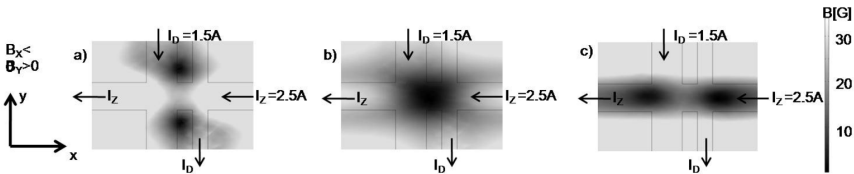


Figure 2: *Magnetic field for different configurations of chip currents and bias fields on a plane $70\mu\text{m}$ below the wires. a) shows $|B_x|/|B_y| = 1.4$, b) $|B_x|/|B_y| = 0.7$, c) $|B_x|/|B_y| = 0.4$*

¹V.A. Prieto and J. Alexander would like to acknowledge support from the U.S. Army Research Laboratory Postdoctoral Fellowship Program administered by Oak Ridge Associated Universities

Atom chip based generation of entanglement for quantum metrology

M.F. Riedel^{1,2}, P. Böhi^{1,2}, Y. Li^{3,4}, T.W. Hänsch^{1,2}, A. Sinatra³, P. Treutlein^{1,2,5}

¹*Fakultät für Physik, Ludwigs-Maximilians-Universität, München, Germany*

²*Max-Planck-Institute for Quantum Optics, Garching, Germany*

³*Laboratoire Kastler Brossel, Paris, France*

⁴*State Key Laboratory of Precision Spectroscopy, Department of Physics, East China Normal University, Shanghai, China*

⁵*Departement Physik, Universität Basel, Basel, Switzerland*

Entanglement-based technologies, such as quantum information processing, quantum simulations, and quantum metrology, have the potential to revolutionize our way of computing and measuring, and help clarify the puzzling concept of entanglement itself. Ultracold atoms on atom chips are attractive for their implementation, as they provide control over quantum systems in compact, robust, and scalable setups. A severe limitation of atom chips, however, is that techniques to control atomic interactions and thus to generate entanglement have not been experimentally available so far.

Here, we present experiments where we generate multi-particle entanglement on an atom chip¹ by controlling elastic collisional interactions with a state-dependent microwave near-field potential². We employ this technique to generate spin-squeezed states of a two-component Bose-Einstein condensate and show that they are useful for quantum metrology. The observed reduction in spin noise combined with the spin coherence imply four-partite entanglement between the condensate atoms and could be used to improve an interferometric measurement over the standard quantum limit. Our data show good agreement with a dynamical multi-mode simulation³ and allow us to reconstruct the Wigner function of the spin-squeezed condensate. The techniques demonstrated here could be directly applied in chip-based atomic clocks which are currently being set up. Furthermore, they constitute the key ingredient for a quantum phase gate which was previously proposed⁴.

¹M. F. Riedel et al. Atom chip based generation of entanglement for quantum metrology, *Nature*, Advanced Online Publication, DOI: 10.1038/nature08988

²P. Böhi et al. Coherent manipulation of Bose-Einstein condensates with state-dependent microwave potentials on an atom chip. *Nat. Phys.* **5**, 592 (2009).

³Y. Li, P. Treutlein, J. Reichel, A. Sinatra. Spin squeezing in a bimodal condensate: spatial dynamics and particle losses. *Eur. Phys. J. B* **68**, 365-381 (2009).

⁴P. Treutlein et al. Microwave potentials and optimal control for robust quantum gates on an atom chip. *Phys. Rev. A* **74**, 022312 (2006).

The Atomic Coherence Population Control Using Stimulated Raman Transitions

Z.Y. Wang, B. Cheng, S.L. Han, T.J. Tao, J.F. Zhang, B. Wu, L.L. Zheng, C.X. Xie, Y.F. Xu, Q. Lin

Institute of Optics, Department of Physics, Zhejiang University, Hangzhou, China

Among many applications in atom optics, we will focus on atom interferometer. By using the precise control of the Raman laser pulses in time and space, the coherent ultracold atom wave packet is splitted, combined, and then re-splitted in the process¹. Then the atomic wave packet will acquire different phase because of the different evolution path. Meanwhile, the matter wave packets in the different evolution path will bring the information of the outside field, so the field information can be deduced through the precision measurement of atomic interference fringes phase.

We first trapped Rubidium (⁸⁷Rb) atoms in a MOT, with its number up to 4×10^9 and its temperature down to $10 \mu K$ after a molasses stage of 6ms. We have studied the Stimulated Raman spectrum between the ground levels ($5^2S_{1/2}F = 1 \rightarrow 5^2S_{1/2}F = 2$) of these atoms after free falling of few tens of milliseconds. The available transitions are three velocity insensitive transitions ($F = 1 \rightarrow F = 2, \Delta m_F = 0$) and other two copies of these transitions Doppler shifted according to the different laser propagating direction related to atoms. In our experiment condition, the total power of Raman laser is about 40mW, Raman beam diameter of 20mm, we have measured velocity sensitive Rabi Oscillation of angle frequency 110kHz and π transition length $28 \mu s$. Following the state preparation, a $\pi/2-\pi-\pi/2$ pulse sequence with interrogation time of up to 180ms has been applied to atoms to form an interferometer. We measured the population of states output from the interferometer using retro-reflected laser beams perpendicular to the atom falling direction and collecting fluorescence from different region using lens and photodiodes. Scanning the Raman laser frequency ramp rate, we got a series of Ramsey fringes of different interrogation times. At interrogation time of 80ms, the Ramsey fringes had the contrast of 16% and phase uncertainty of 100mrad after average of 100 shots.

This work was supported by the National Natural Science Foundation of China (60925022 & 10804097), the Zhejiang Provincial Qian-Jiang-Ren-Cai Project of China (2009R10034), the Research Fund for the Doctoral Program of Higher Education of china (20090101120009) and the Fundamental Research Funds for the Central Universities (2009QNA3024).

¹M. Kasevich and S. Chu, "Atomic Interferometry Using Stimulated Raman Transition", Phys. Rev. Lett., 67(2):181-184, 1991.

Measurement of local gravity via a cold atom interferometer

Lin Zhou^{1,2,3}, Peng Xu^{1,2,3}, Zongyuan Xiong^{1,2,3}, Wei Yang^{1,2,3}, Biao Tang^{1,2,3},
Wencui Peng^{1,2,3}, Yibo Wang^{1,2,3}, Jin Wang^{1,2}, Mingsheng Zhan^{1,2,*}

¹State Key Laboratory of Magnetic and Atomic and Molecular Physics, Wuhan Institute of Physics and Mathematics, Chinese Academy of Sciences - Wuhan National Laboratory for Optoelectronics, Wuhan 430071, China

²Center for Cold Atom Physics, Chinese Academy of Sciences, Wuhan 430071, China

³Graduate University of the Chinese Academy of Sciences, Beijing 100049, China

*corresponding author: mszhan@wipm.ac.cn

We demonstrated a precision measurement of local gravity acceleration g in Wuhan by a compact cold atom interferometer. The atom interferometer is in vertical Mach-Zehnder configuration realized using a $\pi/2 - \pi - \pi/2$ Raman pulse sequence. Cold atoms were prepared in a magneto-optical trap, launched upward to form an atom fountain, and then coherently manipulated to interfere by stimulated Raman transition¹. Population signal vs. Raman laser phase was recorded as interference fringe, and the local gravity information was deduced from the interference signal. We have obtained a resolution of 7×10^{-9} g after an integration time of 236 s. The tidal phenomenon was observed by continuously monitoring the local gravity over 123 hours.

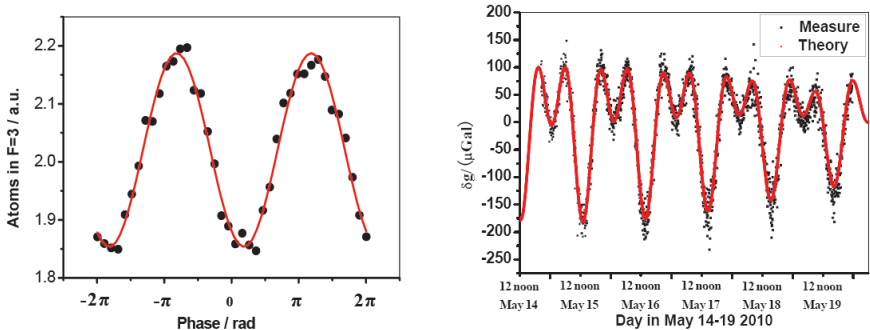


Figure 1: (a) Interference fringes exhibited as a function of relative population to the phase of Raman lasers. Interrogation time between pulses is $T=150$ ms, 4 times average in 236s, (b) 123 hours gravity data measured at Wuhan from May 14 to May 19, 2010.

¹A. Peters, K.Y. Chung, and S. Chu, Nature **400**, 849(1999).

Fine-structure energy levels, oscillator strengths and lifetimes in Si-like Copper

G. P. Gupta¹, A. Z. Msezane²

¹*Department of Physics, S. D. (Postgraduate) College, Muzaffarnagar - 251 001, (Affiliated to Chowdhary Charan Singh University, Meerut - 250 004), INDIA*

²*Department of Physics and Center for Theoretical Studies of Physical Systems, Clark Atlanta University, Atlanta, Georgia 30314, USA*

Emission lines due to allowed and intercombination transitions in multiply charged Si-like ions are observed in solar corona and laser produced plasma. The lines arising from intercombination transitions have been shown to be very useful, for instance, in understanding density fluctuations and elementary processes which occur in both interstellar and laboratory plasma and the determination of transition energies, oscillator strengths and transition probabilities of these lines as needed for a qualitative analysis of the spectra are not well known. This is mainly because these weak lines are usually sensitive to the theoretical modeling and have been a challenge for the atomic structure theory.

Large scale CIV3 calculations of excitation energies from ground state as well as of oscillator strengths and radiative decay rates for all electric-dipole-allowed and intercombination transitions among the fine-structure levels of the terms belonging to the $(1s^2 2s^2 2p^6) 3s^2 3p^2, 3s 3p^3, 3p^4, 3s^2 3p 3d, 3p^3 3d, 3s 3p 3d^2, 3s^2 3d^2, 3s 3p^2 3d, 3s 3p^2 4s, 3s^2 3p 4s, 3s^2 3p 4p, 3s^2 3p 4d$ and $3s^2 3p 4f$ configurations of Si-like Copper, are performed using very extensive configuration-interaction (CI) functions¹. The relativistic effects in intermediate coupling are incorporated by means of the Breit-Pauli Hamiltonian². The errors, which often occur with sophisticated *ab initio* atomic structure calculations, are reduced to a manageable magnitude by adjusting the diagonal elements of the Hamiltonian matrices. In this calculation we have investigated the effects of electron correlations on our calculated data, particularly on the intercombination transitions, by including orbitals with up to $n=5$ quantum number. We considered up to two electron excitations from the valence electrons of the basic configurations and included very large number of configurations to ensure convergence.

Our calculated excitation energies, including their ordering, are in excellent agreement with the experimentally compiled energy values of the National Institute for Standards and Technology (NIST), wherever available. The mixing among several fine-structure levels is found to be very strong. These levels are identified by their eigenvector composition³. From our radiative rates, we have also calculated the radiative lifetimes of the fine-structure levels. Our calculated lifetime for the level $3s 3p^3(^5S_2)$ is found to be in excellent agreement with the experimental results of Trabert et al.⁴.

¹A. Hibbert, *Comput. Phys. Commun.* **9**, 141 (1975)

²R. Glass, A. Hibbert, *Comput. Phys. Commun.* **16**, 19 (1978)

³G. P. Gupta, K. M. Aggarwal, A. Z. Msezane, *Phys. Rev.* **A70**, 036501 (2004); K. M. Aggarwal, Vikas Tayal, G. P. Gupta, F. P. Keenan, *Atom. Data Nucl. Data Tables* **93**, 615 (2007)

⁴E. Trabert et al., *J. Opt. Soc. Am. B* **5**, 2173 (1988)

Measuring the Nuclear Magnetic Octupole Moment of Barium-137

A. Kleczewski, M. Hoffman, E. Magnuson, B.B. Blinov, E.N. Fortson

University of Washington, Seattle, Washington, USA

Measurements of hyperfine structure in the cesium-133 atom resolved a nuclear magnetic octupole moment (Ω) much larger than expected from the nuclear shell model¹. To explore this issue further, we are undertaking an experiment to measure the hyperfine structure in the 5D manifold of a single trapped barium-137 ion which, together with reliable calculations in alkali-like Ba+, should resolve Ω with sensitivity better than the shell model value². We use a 2051 nm TmHo:YLF laser and a 1762 nm fiber laser to drive the $6S_{1/2}$ to $5D_{3/2}$ and $6S_{1/2}$ to $5D_{5/2}$ electric quadrupole transitions. These lasers allow us to selectively populate any hyperfine sub-level in the 5D manifold. We then perform RF spectroscopy to determine the splittings between the $m=0$ sublevels of each hyperfine state.

¹V. Gerginov, A. Derevianko, and C. E. Tanner, Phys. Rev. Lett. 91, 072501

²K. Beloy, A. Derevianko, V. A. Dzuba, G. T. Howell, B. B. Blinov, E. N. Fortson, arXiv:0804.4317v1 [physics.atom-ph] 28 Apr 2008

Stark shift of the Cs clock transition frequency: A CPT-pump-probe approach

J.-L. Robyr, P. Knowles, A. Weis

Department of Physics, University of Fribourg, Fribourg, Switzerland

The Stark effect describes the shift of atomic energy levels by an external electric field. In Cs atomic clocks, the AC Stark shift caused by the blackbody radiation is an important source of systematic frequency shifts. We are currently using a fully optical Raman-Ramsey pump-probe experiment on a thermal Cs atomic beam to perform a precise measurement of the Cs ground state electric polarizability which describes the Stark shift. We expected accuracy below 1%.

The experimental scheme is similar to that of Cs atomic beam clocks except that the microwave cavities are replaced by a coherent population trapping (CPT) interaction. The interference signal obtained in this configuration produces a Ramsey fringe pattern as a function of the Raman detuning. Measuring the shift of the central Ramsey fringe, as induced by an applied static electric field in the free evolution zone, allows the DC Stark shift to be extracted.

The dependence of the clock frequency shift on the applied capacitor voltage has been successfully measured for the $\Delta m = 0, F = 3 \rightarrow F = 4$ hyperfine ground states transitions. The difficult task of the calibration of the electric field and the experimental geometry will be presented and discussed.

Work funded by the Swiss National Science Foundation, #200020–126499.

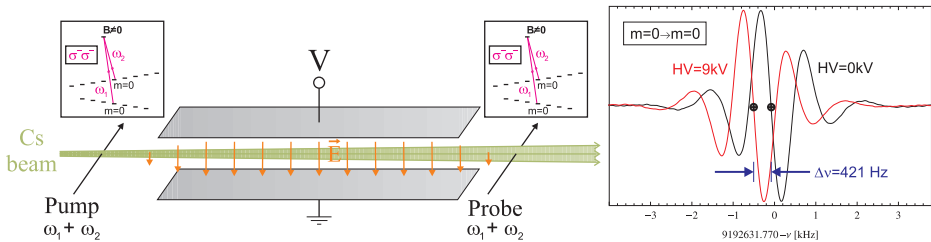


Figure 1: *Left: CPT-Ramsey interrogation scheme for the Stark shift measurement. The Stark shift induced in the atomic coherence by the static electric field is probed by the same bichromatic light field creating a Ramsey interference. Right: Typical Stark shift induced in the Ramsey interference by a 9 kV voltage applied to the electrodes.*

Blackbody Radiation Shifts and Magic Wavelengths for Atomic Clock Research

M.S. Safronova¹, M.G. Kozlov², Dansha Jiang¹, U.I. Safronova³

¹*University of Delaware, Newark, USA*

²*PNPI, Russia*

³*University of Nevada, Reno, USA*

The operation of atomic clocks is generally carried out at room temperature, whereas the definition of the second refers to the clock transition in an atom at absolute zero. This implies that the clock transition frequency should be corrected in practice for the effect of finite temperature of which the leading contributor is the blackbody radiation (BBR) shift. Experimental measurements of the BBR shifts are difficult.

We developed a theoretical method within the framework of relativistic many-body theory to accurately treat correlation corrections in atoms with few valence electrons. This method combines the all-order approach currently used in precision calculations of properties of monovalent atoms with the configuration-interaction approach that is applicable for many-electron systems. This approach has been tested on the calculation of energy levels of divalent systems from Mg to Hg. We have demonstrated an improvement of at least a factor of 3 in agreement with experimental values for the two-electron binding energies and most excited-state energies in comparison with the CI+MBPT (many-body perturbation theory) method [1]. In the present work, we have extended CI+all-order method to the calculation of the transition properties and polarizabilities of divalent systems. Results are reported for the blackbody radiation shifts and magic wavelengths of divalent systems that are of interest to atomic clock development.

We also calculated the blackbody radiation shift of the ground-state hyperfine microwave transition in ⁸⁷Rb using the relativistic all-order method and evaluated the accuracy of our final value. Particular care is taken to accurately account for the contributions from highly-excited states. Our predicted value, $-1.240(4) \times 10^{-10}$ Hz/(V/m)² is three times more accurate than the previous calculation. Various Rb atomic properties, including E1, E2, and E3 ground state polarizabilities, *np* and *nd* E1 polarizabilities, and hyperfine constants are also calculated. The results are compared with experiment and other theory where available.

[1] M.S. Safronova, M. G. Kozlov, W.R. Johnson, Dansha Jiang, Phys. Rev. A 80, 012516 (2009).

Measurements in an optical lattice clock

A. Ludlow¹, N. Lemke¹, Y Jiang^{1,2}, J. Sherman¹, C. Oates¹

¹*National Institute of Standards and Technology, Boulder, CO, USA*

²*Present affiliation: Eastern Chinese Normal University, Shanghai, China*

We report recent measurements of an optical atomic clock based on ^{171}Yb atoms tightly confined in an optical lattice potential. Optical lattice clocks have already demonstrated performance rivaling cesium primary standards, and these young systems have further potential to be realized. We describe measurements made with atoms confined in both one dimensional and two dimensional lattices. For the two dimensional lattice confinement, we explore polarization effects as they couple to the lattice induced vector Stark shift. In both the 1-D and 2-D lattice cases, we study the effect of cold collisions on the clock transition frequency. In particular, using Ramsey interrogation of the clock transition, where the atomic excitation is roughly constant during the long dark time, we study the collisional shift as a function of excitation. We observe a clear zero crossing in the shift near 50% excitation as well as the presence of inelastic decay mechanisms. These measurements will be discussed in more detail.

We also describe improvements to the measurement instability of the Yb clock, where effort has focused on reducing the frequency noise of the probing laser used as the local oscillator. We demonstrate laser instability below the 4×10^{-16} level at short time scales. We also demonstrate how these systems can be designed and constructed with a zero crossing in the coefficient of thermal expansion at temperatures above the ambient room environment.

Finally, we also discuss upcoming plans to help reduce the Stark shift uncertainty from blackbody radiation.

Short-term stability improvements of an optical frequency standard based on free Ca atoms

J. Sherman, C. Oates

National Institute of Standards and Technology, Boulder, CO, USA

Compared to optical frequency standards featuring trapped ions or atoms in optical lattices, the strength of a standard using freely expanding neutral calcium atoms is not ultimate accuracy but rather short-term stability and experimental simplicity. Recently, a fractional frequency instability of 4×10^{-15} at 1 second was demonstrated for the Ca standard at 657 nm¹. The short cycle time (~ 3 ms) combined with only a moderate interrogation duty cycle ($\sim 15\%$) is thought to introduce excess, and potentially critically limiting technical noise due to the Dick effect—high-frequency noise on the laser oscillator is not averaged away but is instead down-sampled by aliasing. We investigated two strategies to minimize this effect: the reduction of clock laser noise by filtering the master clock oscillator through a high-finesse optical cavity² and an optimization of the interrogation cycle to match our laser's noise spectrum.

We have found that optically filtering the clock laser reduced the total Dick effect by approximately one third, and that the Dick effect accounts for approximately half of the clock's instability at 1s. We were not able to optimize the clock's cycle time to observably increase stability. Cavity noise, due to white frequency fluctuations and vibrations, dominate the instability budget. We will present several techniques developed to determine the various instability contributions without making use of an independent clock laser or a fs-comb.

¹Oates et al., *Optics Letters*, **25**(21), 1603–5 (2000)

²Nazarova et al., *J. Opt. Soc. Am. B*, **5**(10), 1632–8 (2008)

Interaction-induced suppression of collisional shifts in a Sr-87 optical lattice clock

M.D. Swallows, M. Bishoff, Y. Lin, S. Blatt, M.J. Martin, A.M. Rey, J. Ye

JILA, NIST, and University of Colorado

Optical atomic clocks based on ensembles of neutral alkaline earth atoms trapped in a magic wavelength optical lattice are promising candidates for the future generation of frequency standards¹. One advantage of neutral atom clocks is the simultaneous interrogation of a large number of atoms, which can in principle allow them to surpass the stability achievable with clocks based on single ions. However, several obstacles must be overcome before this advantage can be realized. One of these is atomic density-dependent collisional shifts of the clock transition, which can occur even if the clock is based on an ensemble of ultracold fermions polarized to a single magnetic sublevel². We have greatly reduced the collisional shift in the JILA ⁸⁷Sr optical lattice clock by trapping atoms in a two-dimensional optical lattice. We exploit a novel quantum many-body effect to suppress collisional shifts in lattice sites containing $N > 1$ atoms. Counter-intuitively, if the interatomic interactions can be made strong enough, collisional shifts of the clock transition are suppressed by the interactions themselves. We have made a high-precision measurement of these effects, and we find that the collisional shift in our 2D lattice clock is $4.0 \pm 1.7 \times 10^{-17}$ at normal operating densities. We will report on this and other developments with the JILA lattice clock, including progress towards eliminating the frequency shifts due to blackbody radiation by trapping atoms inside a cryogenically shielded region.

¹A. D. Ludlow *et al.*, Science, **319**(5871) pp. 1805-1808, 2008.

²G. K. Campbell *et al.*, Science, **324**(5925) pp. 360-363, 2009.

Frequency comparison between two optical lattice clocks towards 10^{-16} uncertainty

T. Takano^{1,3}, M. Takamoto^{2,3}, H. Katori^{2,3}

¹*Photon Science Center, School of Engineering, The University of Tokyo, Japan*

²*Department of Applied Physics, School of Engineering, The University of Tokyo, Japan*

³*CREST, Japan Science and Technology Agency, Saitama, Japan*

Optical lattice clocks¹ interrogate millions of atoms trapped in the Lamb-Dicke regime of optical lattices, which suppresses the Doppler shift and may overcome the quantum projection noise limited stability of singly trapped ion based clocks. The use of many atoms, in turn, may introduce collisional frequency shift, which is a major challenge for the lattice clock. For fermionic atoms, collision suppression by Pauli blocking has been explored by using spin-polarized ⁸⁷Sr atoms in a 1D optical lattice². Alternatively, atoms may be trapped in a single occupancy 3D lattice, which is applicable to bosonic atoms. Recently, we have demonstrated a 3D lattice clock based on bosonic ⁸⁸Sr atoms³ in addition to a 1D lattice clock with spin-polarized fermionic ⁸⁷Sr. The Allan deviation calculated from the beat note of the two clocks reached less than 5×10^{-16} for an averaging time of 2000 s.

In this poster, we report a recent optimization of the experimental scheme which improved the relative stability up to 1×10^{-16} for an averaging time of 1350 s. This improvement allowed us better evaluation of the frequency uncertainty of the 3D bosonic optical lattice clock by referencing the 1D lattice clock with ⁸⁷Sr. To suppress the uncertainty to 10^{-16} , we improved the stability of the bias magnetic field, the lattice frequency, and the probe laser intensity. Furthermore, we canceled the Doppler shift caused by the motion of the reflecting mirror of the optical lattice by stabilizing the relative phase of the probe light to the mirror surface. By these improvements, the total schematic uncertainty is expected to be suppressed to 8×10^{-16} . This research was supported by Advanced Photon Science Alliance (APSA).

¹H. Katori et al., Phys. Rev. Lett. 91, 173005 (2003).

²M. Takamoto et al., J. Phys. Soc. Jpn. 78, 013301 (2009).

³T. Akatsuka et al., Nat. Phys. 4, 954 (2008).

High harmonic generation toward direct excitation of atomic transitions in VUV

Kentarō Wakui¹, Kazuhiro Hayasaka¹, and Tetsuya Ido^{1,2}

¹*National Institute of Information and Communications Technology,
4-2-1 Nukui-kitamachi, Koganei, Tokyo, 184-8795, Japan*

²*PRESTO, Japan Science and Technology Agency*

Dehmelt proposed an optical clock with a fractional uncertainty of 10^{-18} level based on trapped ions with rare-earth metal electron structures in 1982¹. However, the $^1S_0 - ^1P_1$ transitions used for state detection of these ions are typically found in the vacuum ultraviolet (VUV) region, which cannot be accessed by conventional frequency up-conversion techniques using nonlinear crystals. It has thus far been difficult to directly implement his proposal, while the difficulty was detoured by quantum logic spectroscopy which realized the most accurate clock to date². In addition, serious discussions and experimental effort toward optical clocks based on a nuclear transition have lately started, where the clock transition is also expected to be located in 150-190 nm VUV region³.

Coherent VUV radiation has been mostly realized by high harmonic generation (HHG) of near infrared (NIR) pulses obtained by chirped pulse amplifiers. Passive enhancement and HHG of NIR pulses using a buildup cavity, on the other hand, were developed in 2005⁴ and the harmonics have reached the extreme UV region. Considering to use this VUV radiation to the spectroscopy of In^+ , the $^1S_0 - ^1P_1$ transition at 159 nm can be generated as the 5th harmonic of 795 nm, where the maximum intensity of titanium sapphire (Ti:S) lasers is available. Based on this argument as well as the future possibility to study narrow atomic or nuclear transition in VUV, we have aimed to produce the cavity-based HHG of NIR pulses generated by a tunable Ti:S oscillator.

In our experimental setup, a Ti:S laser generates 60 fsec pulses at the fundamental wavelength of 795 nm. Matching the repetition frequency (112 MHz) to a passive optical ring cavity, NIR pulses are built up 350 fold with a coupling bandwidth of 15 nm. This corresponds to an intracavity averaging intensity of 250 W, and the peak intensity at the focus (10 μm) is estimated to be in the order of $10^{13} \text{W}/\text{cm}^2$. When xenon gas jet was provided at the tight cavity focus, fluorescent plasma was clearly observed via multiphoton ionization. At an electrode placed to gather ionized Xe atoms, the plasma current was measured to be more than 3 μA with the nozzle backing pressure of 1000 mbar. Higher order harmonics are outcoupled at a "diffraction grating mirror"⁵ which is inserted right after the gas jet, and then impinge on a fluorescence plate. High harmonics including the 5th harmonic were observed on the plate.

¹Dehmelt, IEEE Trans. IM- **31**, 83 (1982).

²Chou et al., Phys. Rev. Lett. **104**, 070802 (2010).

³Peik and Tamm, Europhys. Lett. **61**, 181 (2003); Campbell et al., Phys. Rev. Lett. **102**, 233004 (2009).

⁴Jones et al., Phys. Rev. Lett. **94**, 193201 (2005); Gohle et al., Nature **436**, 234 (2005).

⁵Yost et al., Opt. Lett. **33**, 1099 (2008).

Laser Cooling and Trapping in Ytterbium Optical Clocks

X. Xu, W. Wang, G. Li, Q. Zhou H. Jiang

State Key Laboratory of Precision Spectroscopy and Department of Physics, East China Normal University, Shanghai 200062, China

The experiments on laser cooling and trapping of ytterbium atoms are reported, including the two-dimensional transversal cooling, the longitudinal velocity Zeeman deceleration, the broadband Doppler-cooling at the 399-nm transition and the narrowband Doppler-cooling at the 556-nm transition. Cold ytterbium atoms have been produced with the number of about ten millions and temperature of a few tens micro-Kelvin. In addition, the experiments on loading ytterbium atoms in a 3D optical lattice are also discussed. Furthermore, we are going to investigate the ultranarrow-linewidth clock transition of cold ytterbium atoms in the optical lattice with an Hz-level-linewidth probe laser. Ultimately, an ytterbium optical clock will be developed.

References 1. M. Takamoto, F. Hong, R. Higashi, and H. Katori, *Nature* 435, 321(2005) 2. Z.W. Barber, J. E. Stalnaker, N. D. Lemke, N. Poli, C. W. Oates, T. M. Fortier, S. A. Diddams, L. Hollberg, and C. W. Hoyt, A. V. Taichenachev, and V. I. Yudin, *Phys. Rev. Lett.*, 100, 103002(2008)

Spectroscopy of the ^{87}Sr Clock Transition toward an Optical Lattice Clock

A. Yamaguchi^{1,2}, N. Shiga³, S. Nagano^{1,2}, H. Ishijima¹, M. Hosokawa¹, T. Ido^{1,2}

¹*National Institute of Information and Communications Technology, Tokyo, Japan*

²*CREST, Japan Science and Technology Agency, Japan*

³*PRESTO, Japan Science and Technology Agency, Japan*

At NICT, we started to build an ^{87}Sr optical lattice clock in 2006. Recently, we have loaded ultracold ^{87}Sr atoms into a one dimensional (1D) optical lattice and performed a high resolution spectroscopy of the $^1S_0 - ^3P_0$ clock transition.

Strontium atoms are first cooled and trapped in a magneto-optical trap (MOT) using the strong $^1S_0 - ^1P_1$ ($\lambda = 461$ nm) transition. The atoms are further cooled by the second MOT using the narrower $^1S_0 - ^3P_1$ ($\lambda = 689$ nm) transition and loaded in a 1D optical lattice potential at the magic wavelength ($\lambda = 813$ nm). The tight confinement of the lattice potential enables us to carry out the spectroscopy of the $^1S_0 - ^3P_0$ ($\lambda = 698$ nm) clock transition in the Lamb-Dicke regime. We used an external cavity diode laser to excite the clock transition. The laser frequency is first locked to a prestabilization cavity and then stabilized to a high finesse cavity (Finesse = 200 000). The fractional instability of the cavity-stabilized clock laser is 1×10^{-14} at 1 s. In a longer averaging time, the instability is kept below 1×10^{-14} until 100 s. Further improvement is in progress to reach the thermal-noise limited regime.

We carried out the absolute frequency measurement of the clock transition referred to UTC(NICT). The measurement agreed with the CIPM recommended frequency within the 1σ error of our measurement. Currently, the statistical uncertainty reaches 7×10^{-15} . The systematic uncertainty is limited to 30 Hz (7×10^{-14}) because our own magic wavelength and corresponding ac Stark shift coefficient has not been precisely evaluated yet. We are in a process of reducing systematic errors, including the direct comparison between the Sr optical lattice clock and our Cs fountain (NICT-CsF1) in order to eliminate the uncertainty related to the UTC(NICT). We are also working toward a frequency comparison between Sr lattice clock in NICT, Sr clocks in University of Tokyo and Sr/Yb clocks in NMIJ/AIST through the fiber-link network around the Tokyo area.

New approaches to an atomic clock based on coherent population trapping.

S.H. Yim, D. Cho

Department of Physics, Korea University, Seoul 136-713, Korea

We employed new approaches to an atomic clock which could operate with neither a local oscillator nor a modulator. First, we developed an atomic clock using two modes from a single extended-cavity diode laser in multimode operation as a quasi-coherent pair of laser beams. We use dispersion of the coherent population trapping (CPT) resonance to obtain an error signal eliminating the need for an extra frequency modulation. The two modes are phase locked with reference to a dispersion signal from a CPT resonance of ^{85}Rb at 3.036 GHz ground hyperfine splitting. We use D1 transition at 794.8 nm with $\text{lin} \perp \text{lin}$ polarizations to obtain large-contrast CPT signal. The beating signal between the two modes is used as a clock output. The design is a significant simplification over a conventional CPT-based atomic clock with a local oscillator. Allan deviation of the beat frequency is 1×10^{-10} at 200-s integration time.

Another scheme to make a CPT atomic clock is an optoelectronic oscillator (OEO) which was first demonstrated by Maleki and company in 1996¹. OEO is a simple photonic device which consists of a laser as a light source, an electro-optic modulator (EOM) to produce a pair of coherent laser beams and a fast photodiode (FPD) to recover the beating signal. The beating signal is amplified and fed back to the EOM. Instead of the phase modulation by an EOM, we use a direct modulation of an injection current of the ECDL. In order to stabilize an OEO loop length, we use the dispersion signal from the CPT resonance. Narrow CPT resonance improves the frequency stability of the OEO by increasing the total OEO loop length as a result of slow light effect. The CPT resonance plays a role of microwave band pass filter as well.

¹X. Steve Yao and Lute Maleki, " Optoelectronic microwave oscillator," J. Opt. Soc. Am. B/Vol. 13, No. 8/August 1996.

Measurement of Charge Exchange Cross Sections for the He^- Production in Li

M. Sasao, T. Nagamura, N. Tanaka, M. Kisaki, K. Terai, A. Okamoto, S. Kitajima

Graduate school of Engineering, Tohoku University, Sendai, Miyagi 980-8579, Japan

An energetic He^0 beam is strongly demanded in alpha particle diagnostics on nuclear fusion experiments^{1 2}. While the electron attachment efficiency of He^+ is very low in the energy region above 1 MeV, the He^0 production by Time-Of-Flight from He^- using the life times ($10\mu\text{sec}$ and $300\mu\text{sec}$) is much easier³.

Figure 1 shows the schematic diagram of the Proof-Of-Principle device of the He^0 TOF production⁴. On this device, He^- is produced in Lithium vapor, which has relatively low efficiency but is the safest alkali metal in handling. The change of the He^- and that of He^+ current were measured as the function the line integrated Lithium density, which was calibrated using the well known electron capture cross section of H^+ . Injection energy of the He^+ was in the range of 8 - 20 keV. Assuming that the He^- is only produced from the He^* triplet state, ^3S , as shown in Figure 2, and that the electron capture cross section ratio from He^+ to the singlet and to the triplet state is 1:3, cross sections of $\sigma(+, ^1\text{S}+^3\text{S})$, $\sigma(^3\text{S}, +)$, $\sigma(^3\text{S}, -)$, $\sigma(^3\text{S}, ^1\text{S})$, $\sigma(-, ^3\text{S})$ were obtained.

Compared with these electron capture/loss cross sections in Cesium vapor⁵, these cross sections are almost same in amplitudes, except $\sigma(^3\text{S}, +)$. The ionization cross section of $\text{He}(^3\text{S})$ in Lithium is about three times larger than those in Cesium. This causes the low, about one order less, He^- production efficiency in Li.

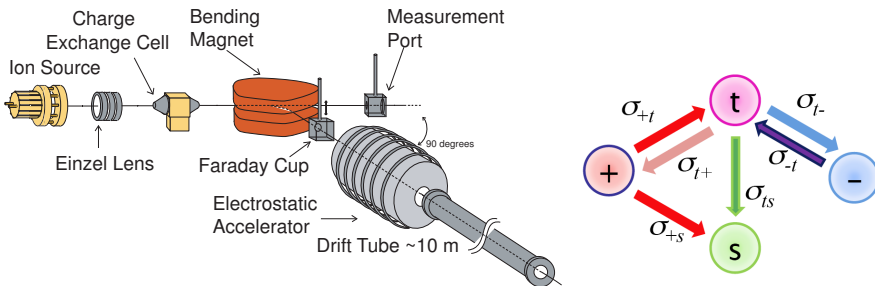


Figure 1: Schematic diagram of POP device. Figure 2: Production scheme of He^- .

¹D. E. Post, et al., J. Fusion Energy, 1, 129 (1981).

²M. Sasao et al., Fusion Technol. 10(1986) 236.

³M. Sasao et al., Rev. Sci. Instrum. 77, 10F130 (2006).

⁴N. Tanaka et al., Plasma Fusion Res. 2 S1105 (2007).

⁵A.S. Schlachter, AIP conf. proc. 111(1984) 300.

Feshbach resonances of trapped ultracold atoms

P.-I. Schneider, Y. V. Vanne, A. Saenz

AG Moderne Optik, Institut für Physik, Humboldt-Universität zu Berlin, Newtonstrasse 15, 12489 Berlin, Germany

Confined ultracold atoms with interactions manipulated by a magnetic Feshbach resonance (MFR) have vast and intriguing applications, e.g., for studying new phases of matter, performing quantum information processing, or simulating condensed-matter Hamiltonians¹. The usual theory of MFRs successfully describes the *free* scattering process which is governed by the *s*-wave scattering length. However, traps imply new boundary conditions leading, e.g., to eigenstates of discrete energy E_i .

We reconsider the scattering process in harmonic traps by applying a two-channel description of an MFR and using the analytically known long-range form of the wave function. This allows to derive an equation for the eigenenergies and to quantify the admixture of the resonant molecular bound state (RBS) that leads to the MFR. The model is successfully verified by a comparison with full multi-channel calculations.

The derived eigenenergy equation allows to define an energy-dependent scattering length in the trap $a_{\text{trap}}(E)$. One of the main results is that $a_{\text{trap}}(E)$ differs severely from the energy-dependent *free*-space scattering length $a_{\text{free}}(E)$ for large background scattering lengths. This indicates that an essential modification of MFRs by the trap can occur.

One of the impacts of the trap is a state-dependent magnetic-field shift of the MFR. Applying the model we were able to quantitatively explain disagreeing resonance positions of ^{87}Rb measured in a relatively weak dipole trap² and in an optical lattice³.

Another intriguing prediction of the model concerns the RBS admixture to eigenstates of the system. In free space the admixture of the RBS to the open channel has its maximum exactly at the resonance. Thereby effects of the RBS can hardly be distinguished from effects due to the scattering length. In traps, however, the magnetic-field position of the maximal RBS admixture can be shifted from the resonance and can be even positioned at vanishing scattering length. The effect is best observable for high lying trap levels and large background scattering lengths. An experiment by Bourdel *et al.*⁴ determined the atom-loss rate of Fermionic ^6Li as a function of the magnetic field. This system has a large background scattering length of $-1405 a_0$ and atoms at the Fermi edge occupy high lying trap levels. Accordingly, the model predicts a considerable shift of -83.8 G of the maximal RBS admixture from the resonance. Exactly in this magnetic field region Bourdel *et al.* observed a *global* maximum of atom loss. This indicates that for ^6Li not the scattering length but the RBS plays a dominant role in atom-loss processes.

We acknowledge financial support of the *Deutsche Forschungsgemeinschaft* and the *Deutsche Telekom Stiftung*.

¹D. Jaksch and P. Zoller, *Annals of Physics*, **315**, 52–79 (2005)

²M. Erhard *et al.*, *Phys. Rev. A*, **69**, 032705 (2004)

³A. Widera *et al.*, *Phys. Rev. Lett.*, **92**, 160406 (2004)

⁴T. Bourdel *et al.*, *Phys. Rev. Lett.*, **91**, 020402 (2003)

Enhancement of Rb fine-structure transfer in inert buffer gases due to three-body collisions

J.F. Sell¹, M.A. Gearba², B.M. Patterson¹, T. Genda¹, B. Naumann¹, R.J. Knize¹

¹*Laser and Optics Research Center, U.S. Air Force Academy Department of Physics, USAF Academy, CO 80840 USA*

²*Department of Physics and Astronomy, University of Southern Mississippi, Hattiesburg, MS 39406 USA*

The measurement of fine-structure energy transfer in alkali atoms is one of the older experiments in atomic physics, with the binary (two-body) collisional cross sections having been examined across most of the alkalis with collision partners including the inert and molecular gases¹. Recently experiments using Rb with inert buffer gases observed deviations from the binary collisional cross section, particularly at high buffer gas pressures^{2,3}. We will describe our measurements of Rb $5p$ fine-structure changing collisions in inert gases over a broad range of buffer gas pressures.

Using ultrafast laser excitation and time-correlated single-photon counting techniques we determine the collisional mixing rate from the time-dependence of the observed fluorescence as shown in Fig.1(a). Since the fluorescence from collisional transfer is at a different wavelength than the laser excitation, we reduce scattered laser light along with any polarization effects produced during excitation. As the buffer gas pressure is varied, we observe a nonlinear dependence of the mixing rate with density due to three-body collisions, as shown in Fig.1(b) in the case of ^4He buffer gas. We will also report on experiments in progress with varying buffer gas masses and temperatures.

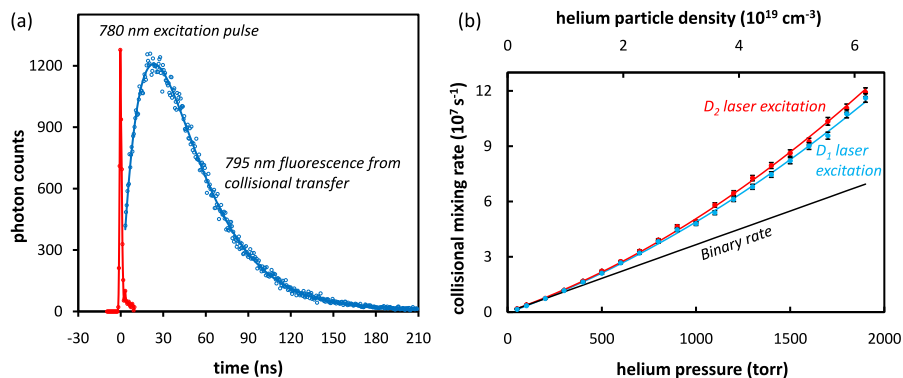


Figure 1: (a) The observed laser pulse along with the fluorescence due to collisional excitation transfer in Rb at a ^4He pressure of 200 torr. (b) The measured $5^2P_{3/2} \rightarrow 5^2P_{1/2}$ collisional mixing rates in Rb at ^4He pressures from 50 to 2000 torr.

¹L. Krause, Adv. Chem. Phys. **28**, 267 (1975)

²K. Hirano, K. Enomoto, M. Kumakura, Y. Takahashi and T. Yabuzaki, Phys. Rev A **68**, 012722 (2003)

³S.S.Q. Wu, T.F. Soules, R.H. Page, S.C. Mitchell, V.K. Kanz and R.J. Beach, Opt. Lett. **32**, 2423 (2007)

Laboratory Astrophysics - Cascade vs. Direct Contributions to the O⁶⁺ on CO Charge-Exchange XUV Emission at Solar Wind Velocities

W.W. Smith¹, K.A. Miller², Q.C. Kessel¹, A. Chutjian³, J. Simcic³, S.J. Smith³,
T. Ehrenreich⁴, C. Verzani⁵

¹*University of Connecticut, Storrs, CT 06269-3046, USA*

²*Columbia University, New York, NY 10027, USA*

³*Jet Propulsion Laboratory/Caltech, Pasadena, CA 48202-3905, USA*

⁴*Nufern Inc., East Granby, CT 06026-9523, USA*

⁵*University of Wisconsin, Stevens Point, WI 54481, USA*

Since the space-based observation of XUV (soft x-ray) radiation from Comet Hyukatake in 1996,¹ similar x rays were seen from all subsequent comets nearing the Sun. Cravens² proposed that the x rays were largely due to bombardment of comet gases (H₂O, CO, CO₂, etc.) by highly-charged, keV-energy minority ions from the solar wind (C^{5,6+}, N^{6,7+}, O^{6,7,8+}, Ne^{q+}, Si^{q+}, Fe^{q+}, etc). Electron transfer (charge exchange) collisions occur from the gas to highly-excited states of the ions. The electrons then cascade down into lower levels, emitting a 0.1 - 10keV soft x-ray line spectrum. The x-ray (SWCX) spectrum correlates well with emission lines of ions; it can be used as a remote diagnostic of comet and solar-wind composition. Spectra from space-based observatories (e.g. Chandra and XMM-Newton) can be compared with theoretical models.^{3 4} Benchmark laboratory measurements help validate these models. We report laboratory simulations of SWCX: collisions of 2.3 keV/amu O⁶⁺ and other ions⁵ on CO gas.⁶ We used JPL's Highly-Charged Ion Facility⁷ and a UConn grazing incidence spectrometer with an XUV CCD camera. Dominant O VI lines indicate capture by the O⁶⁺ into singly excited states of Li-like O⁵⁺, with n = 3, 4 and all allowed l states. The Coulomb over-the-barrier (OBM) model⁸ shows a probability maximum between n=4 and 5, implying the excitation is into the n=4 states. Note that the 17.3 nm line (3d-2p) is too intense to be explained simply by cascade, implying some direct feeding of the n=3 states, not predicted by OBM. We see huge differences between He and CO gas targets. With He, the n=4 lines are suppressed but the n=3l lines are prominent, consistent with the OBM dependence on the target I.P.^{9 10}

¹Lisse, C.M., et al., Science B2 274, 205-209 (1996).

²Cravens, T.E., Science 296, 1042-1045 (2002).

³Kharchenko, V. and Dalgarno, A., J. Geophys. Res. 105, 18351-18,359 (2000).

⁴Bodewits, D., et al., Ap. J. 642, 593 (2006).

⁵Miller, Kenneth A., Ph.D. Thesis, "Collisions of Highly-Charged Solar-Wind Ions with CO", University of Connecticut, Storrs, CT 06269-3046 (2008).

⁶See ICAP 2008 Book of Abstracts, K.A. Miller, et al., p. 251 for more details.

⁷J.B. Greenwood, A. Chutjian, S.J. Smith, Astrophys. J. 259, 605 (2000).

⁸Niehaus, A., J. Phys. B, At. Mol. Phys. 19, 2925 (1986).

⁹A paper by the same authors (K.A. Miller, et al.) is in preparation for submission to Ap. J. (2010).

¹⁰This research was supported in part by NASA grant NCC5-601, and at JPL by agreement with NASA.

Collisional properties of metastable ytterbium atoms

S. Uetake^{1,2}, R. Murakami¹, J.M. Doyle³, Y. Takahashi^{1,2},

¹*Department of Physics, Graduate School of Science, Kyoto University, Kyoto, Japan*

²*CREST, Japan Science and Technology Agency, Tokyo, Japan*

³*Department of Physics, Harvard University, Cambridge, Massachusetts 02138, USA*

Atoms with alkaline-earth electronic structure have shown promise for a number of key applications. In particular, the narrow 1S_0 - 3P_0 resonance of atoms in an optical lattice may be highly competitive as a new frequency standard¹. The use of 3P_0 and 3P_2 states in quantum computing has been explored theoretically with encouraging results². To realize such applications, much more needs to be known about the collisional properties of these species. Here we report the measurement of inelastic collisions of spin-polarized 3P_2 ^{174}Yb atoms confined in a crossed far-off-resonance trap at a temperature of 500 nK.

Atom-atom collisions are observed for several internal Zeeman states. These state-dependent decay curves are presented in the Figure below. We apply a small bias magnetic field to spectroscopically split atoms in different m_J states. Both 3P_2 - 3P_2 and 1S_0 - 3P_2 collision systems are studied. For the 3P_2 - 3P_2 system, the decays are essentially independent of both m_J and magnetic field. For the 1S_0 - 3P_2 system, the behavior is markedly different. First, the overall decay due to 1S_0 - 3P_2 collisions is less rapid than 3P_2 - 3P_2 collisions (see figure caption). Second, the higher Zeeman level 3P_2 atoms ($m_J = 0, +2$) display a strong field dependence in the decay. This clearly and quantitatively shows the important role of Zeeman sublevel changing collisions in the 1S_0 - 3P_2 collision system. Updated results and detailed analysis will be presented.

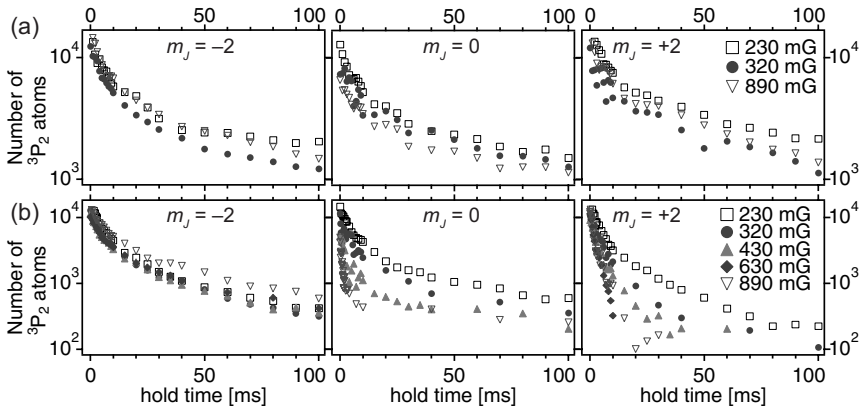


Figure 1: Inelastic losses by collisions between (a) spin polarized 3P_2 atoms; and (b) collisions between 1S_0 and 3P_2 atoms. Note that the number of trapped 1S_0 atoms is ~ 10 times greater than the number of 3P_2 atoms.

¹H. Katori *et al.*, PRL **91**, 173005 (2003)

²K. Shibata *et al.*, Appl. Phys. B **97**, 753 (2009); A. J. Daley *et al.*, PRL **101**, 170504 (2008); A. Derevianko *et al.*, PRA **70**, 062319 (2004); A. V. Gorshkov *et al.*, PRL **102**, 110503 (2009)

First measurement of the Lee-Huang-Yang correction for atomic bosons

R.J. Wild, J.M. Pino, P. Makotyn, E.A. Cornell, D.S. Jin

JILA, Quantum Physics Division, National Institute of Standards and Technology and Department of Physics, University of Colorado

The famous Lee-Huang-Yang (LHY) term describes the first-order correction to the mean-field energy for strongly interacting bosons¹, yet it has only been detected with bosons composed of loosely bound fermion pairs^{2,3}. Tan's universal relations, originally calculated for fermions⁴, connect a property called the Contact to many macroscopic parameters of a quantum gas, such as its total energy. These relations have been verified experimentally for Fermi systems⁵. We apply these relations to a Bose gas to realize a unique tool to measure the LHY correction. We perform RF spectroscopy on a BEC of ⁸⁵Rb close to a Feshbach resonance, and measure the strength of the high-momentum tail which decays as $1/k^4$. From this we extract the Contact, which increases as a function of interaction strength. This provides us with the first observation of the LHY term for atomic bosons and the ability to quantitatively measure the energy of strongly interacting bosons.

¹T. D. Lee, K. Huang, and C. N. Yang, Phys. Rev. **106**, 1135 (1957).

²A. Altmeyer, S. Riedl, C. Kohstall, M. J. Wright, R. Geursen, M. Bartenstein, C. Chin, J. H. Denschlag, and R. Grimm, Phys. Rev. Lett. **98**, 040401 (2007).

³Y. Shin, A. Schirotzek, C. H. Schunk, and W. Ketterle, Phys. Rev. Lett. **101**, 070404 (2008).

⁴S. Tan, Ann. Phys. **323**, 2971 (2008).

⁵J. T. Stewart, J. P. Gaebler, T. E. Drake, and D. S. Jin, arXiv:1002.1987v1 [cond-mat.quant-gas], Phys. Rev. Lett., in press.

Nonsequential Two-Photon Double Ionization of Atoms: Identifying the Mechanism

S.A. Sørngård¹, S. Askeland¹, S. Selstø², R. Nepstad¹, M. Førre¹

¹*Department of Physics and Technology, University of Bergen, Bergen, Norway*

²*Centre of Mathematics for Applications, University of Oslo, Oslo, Norway*

We develop¹ an approximate model for the process of direct (nonsequential) two-photon double ionization of atoms. Employing the model, we calculate (generalized) total cross sections as well as energy-resolved differential cross sections of helium for photon energies ranging from 39 to 54 eV. A comparison with results of *ab initio* calculations reveals that the agreement is at a quantitative level. We thus demonstrate that this complex ionization process is fully described by the simple model, providing insight into the underlying physical mechanism. Finally, we use the model to calculate generalized cross sections for the two-photon double ionization of neon in the nonsequential regime.

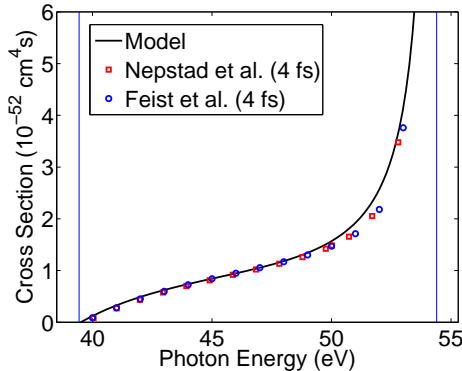


Figure 1: *Total integrated (generalized) cross section for the nonsequential two-photon double ionization of helium. Full line: result obtainthe model; open circles: ab initio result of Feist et al.² obtained with a 4 fs pulse; and open squares: corresponding ab initio result of Nepstad et al.³. The vertical lines define the two-photon direct double ionization region.*

¹M. Førre, S. Selstø and R. Nepstad, submitted to Physical Review

²J. Feist et al., Phys. Rev. A **77**, 043420 (2008)

³R. Nepstad, T. Birkeland and M. Førre, to appear in Phys. Rev. A

Observation of delayed four- and six-wave mixing in a coherently prepared atomic ensemble

D. Felinto, D. Moretti, J. W. R. Tabosa

Departamento de Física, Universidade Federal de Pernambuco, Cidade Universitaria, 50670-901 Recife, PE, Brasil

The coherent atom-light interaction can be used for reversibly store light information into an atomic ground-state coherence. In this work we experimentally demonstrated the observation of higher order wave mixing process in a coherently prepared atomic ensemble. We use a time delayed wave-mixing configuration¹ depicted in Fig. 1(a), (b), where a coherence grating between the Zeeman sublevels of the lower ground state $6S_{1/2}$, $F = 3$ of cold cesium atoms is written by the grating beams W and W' and read a posteriori, after the switching off of the grating beams, using the pair of copropagating reading beams, R and R' . All the beams are circularly polarized with helicities indicated in Fig.1 (a). The two reading pulses couples with the stored Zeeman coherence to induce optical coherences in the transitions coupled by the beams R and R' , which have spatial wavevectors given respectively by $\vec{k}_D = \vec{k}_R + \vec{k}_W - \vec{k}_{W'}$ and $\vec{k}_{D'} = 2\vec{k}_R - \vec{k}_{R'} + \vec{k}_W - \vec{k}_{W'}$, and are associated with the delayed four- and six-wave mixing processes respectively². For the used beam geometry, the corresponding Bragg diffracted signal can be separated using a quarter waveplate and a polarizing beam splitter.

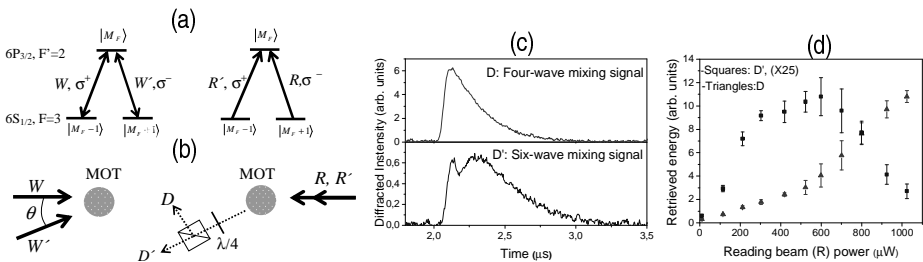


Figure 1: (a) *Generic Zeeman three-level scheme; (b) Writing and reading beams configurations; (c) Diffracted temporal pulse intensities; (d) Diffracted pulse energies as a function of the R beam power for a constant total reading power.*

In Fig. 1 (c) we show the diffracted pulse shape associated with each process and in Fig. 1(d) we plot the diffracted pulse energy for different powers of the reading beam P_R , maintaining constant the total reading beam power, $P_R + P_{R'}$. The different observed pulse shape is a clear evidence of the different mechanism involved in each nonlinear process. Furthermore, the possibility of observing nonlinear interaction between light and coherently prepared atomic ensembles could play an important role for the manipulation of quantum information.

¹D. Moretti, N. Gonzalez, D. Felinto, J. W. R. Tabosa, Phys. Rev.A **78**, 023811 (2008).

²D. Moretti, D. Felinto, J. W. R. Tabosa, Submitted (2010).

Direct simulation of non-adiabatic spin flips and evaporation in a magnetic trap

C. J. Watkins¹, J. Newstead¹, R. P. Anderson¹, J. Z. Liu² and L. D. Turner¹

¹*School of Physics and* ²*Department of Mechanical & Aerospace Engineering, Monash University, Victoria 3800, Australia*

Atomic spins moving in position-dependent magnetic fields are at the heart of many ultracold atomic physics experiments. “Majorana spin flips”, whereby an atom does not remain in a spin eigenstate with respect to its local magnetic field, cause loss from magnetic traps. Though often avoided by various means, they play a larger role in a new form of hybrid trap¹ – comprising a magnetic quadrupole superposed on an optical dipole potential. Previously, the spin-flip mechanism was modelled with a finite sized “hole” from which atoms are expelled from the trap, and analytic estimates for the asymptotic probability of adiabatic following. Instead, we numerically model the coupled spin and motional dynamics of an ensemble of atoms in a magnetic quadrupole field. Directly tracking the spin dynamics provides insight into the spin-flip mechanism and its effect on the velocity distribution of atoms remaining in the trap. Furthermore, we predict interesting behaviour such as trapped atoms exhibiting diabatic following.

In addition, we have modelled rethermalisation of magnetically trapped atoms during forced evaporative cooling using a direct simulation Monte-Carlo procedure.² This approach for handling collisions in particle dynamics is fully compatible with our spin tracking simulations. When combined, these two techniques will allow us to simulate and optimise evaporative cooling in a hybrid trap.^{1,3}

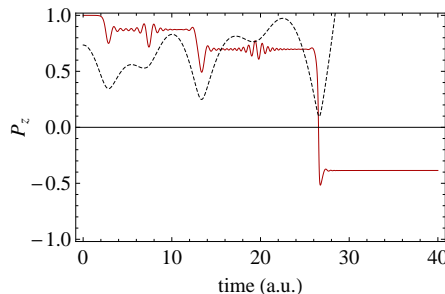


Figure 1: (Solid) Atomic spin projection along the local magnetic field. (Dashed) Radial position of the atomic trajectory (arbitrary units). Initially aligned with the field, the spin partially flips upon approaching the origin, where it imperfectly follows the magnetic quadrupole. After several oscillations in the trap, the spin becomes anti-aligned with the field and it experiences a repulsive force, expelling it from the trap.

¹Y.-J. Lin, A. R. Perry, R. L. Compton, I. B. Spielman and J. V. Porto, *Rapid production of ^{87}Rb BECs in a combined magnetic and optical potential*, Phys. Rev. A **79**, 063631 (2009).

²Huang Wu and C. J. Foot, *Direct simulation of evaporative cooling*, J. Phys. B **29**, L321 (1996).

³Details and code at <http://bec.physics.monash.edu.au/SimulatingSpinsInHybridTraps>

Spatially Resolved Excitation of Rydberg Atoms on an Atom Chip

A. Tauschinsky R. M. T. Thijssen, C. F. Ockeloen, H. B. van Linden van den Heuvell, S. Whitlock, R. J. C. Spreeuw

Van der Waals-Zeeman Institute, University of Amsterdam, The Netherlands

Ultracold atoms excited to high-lying Rydberg states have extremely large transition dipole moments and large electric polarizabilities which allow long-range atom-atom interactions and can greatly enhance atom-surface interactions. We demonstrate spatially resolved, coherent excitation of Rydberg atoms on an atom chip¹. Electromagnetically induced transparency (EIT) is used to investigate the properties of the Rydberg atoms near the gold coated chip surface. We measure distance dependent shifts of the Rydberg energy levels caused by a spatially inhomogeneous electric field. The measured field strength and distance dependence is in agreement with a simple model for the electric field produced by a localized patch of Rb adsorbates deposited on the chip surface during experiments. The EIT resonances remain narrow and the observed widths are independent of atom-surface distance down to $\sim 20\mu\text{m}$, indicating relatively long lifetime of the Rydberg states. Presently we are investigating long-range interactions and collective excitations produced in dense mesoscopic ensembles on the atom chip. Our results are an excellent starting point for further studies of atom-surface interactions, many-body physics and quantum information science involving interacting Rydberg excited atoms on atom chips.

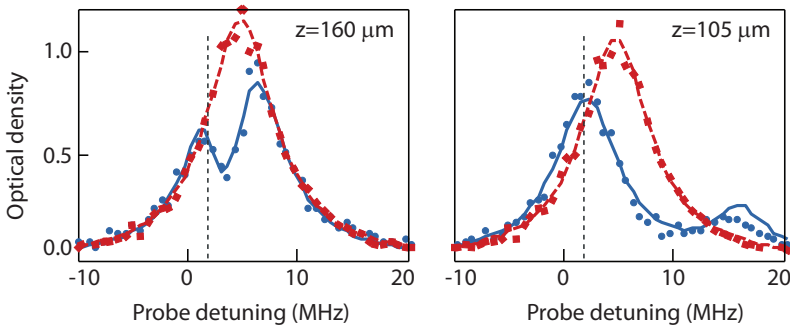


Figure 1: *Optical spectra with coupling to the $36d_{5/2}$ Rydberg state. Circles and squares show the measured probe spectrum with and without the coupling laser respectively. Atom-surface distances of $160\ \mu\text{m}$ (left) and $105\ \mu\text{m}$ (right).*

¹A. Tauschinsky *et al*, Phys. Rev. A. Accepted (2010), preprint arXiv:1004.3230

On the order of BEC transition in weakly interacting gases as predicted by mean-field theory

V. Romero-Rochín, L. Olivares-Quiroz

*Instituto de Física, Universidad Nacional Autónoma de México
Apartado Postal 20-364, México D. F. 01000, Mexico.*

The predictions of Hartree-Fock (HF), Popov (P), Yukalov-Yukalova (YY) and t -matrix (TM) approximations regarding the transition from normal to BEC phase in weakly interacting Bose gases are reviewed. By analyzing the dependence of the chemical potential μ on temperature T and particle density ρ , we show that none of them predicts a second-order phase transition as required by general symmetry considerations. We find that the isothermal compressibility κ_T predicted by these descriptions does not diverge at criticality as expected in a true second-order phase transition. Moreover, the isotherms $\mu = \mu(\rho, T)$ typically exhibit non-single-valued behavior in the vicinity of the BEC transition, a feature forbidden by general thermodynamic principles. This behavior can be avoided by appealing to a first-order phase transition instead. These facts show that although these mean field approximations give correct results near zero temperature, they are endowed with anomalies in the vicinity of the BEC transition. We address the implications of these results in the interpretation and understanding of phenomena in the current experiments with ultracold trapped alkali gases.

Vortex dynamics in a warm Bose-Einstein condensate

S. J. Rooney, A. S. Bradley, P. B. Blakie

Jack Dodd Centre for Quantum Technology, Department of Physics, University of Otago, Dunedin, New Zealand.

Bose-Einstein condensates (BECs) present a unique opportunity for developing *ab initio* theory that can be directly compared to experiments. However, in the area of nonequilibrium dynamics most quantitative comparisons have been limited to the zero temperature regime, where the Gross-Pitaevskii equation provides a comprehensive treatment. In the high temperature regime where $\hbar\omega \ll k_B T$, a more sophisticated approach is necessary to account for the spontaneous and incoherent processes that arise.

In this work we use the stochastic projected Gross-Pitaevskii equation (SPGPE) to quantitatively study the dynamics of quantized vortices in high temperature BECs. The SPGPE is a c-field theory¹, where the modes of system is divided into two regions according to occupation. The highly occupied (low energy) coherent (C) region is described by a classical field using the truncated Wigner method, while the incoherent region (I) with low occupation is treated semiclassically, playing the role of a thermal reservoir at temperature T and chemical potential μ . The SPGPE is given by:

$$d\psi_{\mathbf{C}}(\mathbf{x}, t) = \mathcal{P}_{\mathbf{C}} \left\{ -\frac{i}{\hbar} L_{\mathbf{C}} \psi_{\mathbf{C}}(\mathbf{x}, t) dt + \frac{\gamma}{k_B T} (\mu - L_{\mathbf{C}}) \psi_{\mathbf{C}}(\mathbf{x}, t) dt + dW_{\gamma}(\mathbf{x}, t) \right\}$$

where $\mathcal{P}_{\mathbf{C}}\{\}$ projects the evolution onto the highly occupied C region modes, $L_{\mathbf{C}}$ is the Hamiltonian evolution operator for the C region, the complex noise is given by $\langle dW_{\gamma}^*(\mathbf{x}, t) dW_{\gamma}(\mathbf{x}', t) \rangle = 2\gamma \delta_{\mathbf{C}}(\mathbf{x}, \mathbf{x}') dt$, and γ represents damping induced by collisions between atoms in the C and I regions. The SPGPE gives a non-perturbative description of the interaction between the condensate and thermal atoms.

We use the SPGPE to investigate the dynamics of a centrally located single vortex for a range of temperatures and condensate geometries. We show the major effect the stochastic approach has at high temperatures, and investigate the effect geometry has on the three dimensional structure and dynamics of the vortex.

Further, we model the vortex dipole formation experiment of Neely *et al.*², and calculate the lifetime of the dipole. Using previous methods³ we can determine appropriate SPGPE parameters which lead to the desired total atom number and temperature of the system, and enabling us to calculate the damping rate (γ). Our calculations show quantitative agreement of vortex decay with experiment without fitting any parameters.

¹Dynamics and statistical mechanics of ultra-cold Bose gases using c-field techniques, P. B. Blakie, A. S. Bradley, M. J. Davis, R. J. Ballagh, and C. W. Gardiner, *Adv. in Phys.*, **57**, 363 (2008)

²Observation of Vortex Dipoles in an Oblate Bose-Einstein Condensate, T. W. Neely, E. C. Samson, A. S. Bradley, M. J. Davis, and B. P. Anderson, *Phys. Rev. Lett.*, **104**, 160401 (2010)

³Decay of a quantum vortex: Test of nonequilibrium theories for warm Bose-Einstein condensates, S.J. Rooney, A. S. Bradley, and P. B. Blakie, *Phys. Rev. A*, **81**, 023630 (2010)

Wavepacket engineering of textures in pseudospin BECs

G. Ruben

School of Physics, Monash University, Victoria 3800, Australia

Topological spin textures in pseudospin Bose-Einstein condensates (BECs) are associated with the existence of vortices in the individual spinor components. We have previously shown that interference of three initially separated scalar BEC wavepackets generates a ballistically expanding, two-dimensional nonrotating lattice of singly-quantized vortices and antivortices.¹ By forming two of these lattices in a two-component BEC, a corresponding expanding lattice-texture is formed. Control over the relative phase of the initial BEC wavepackets allows the resulting textures in the lattice motif to be determined *a priori*.²

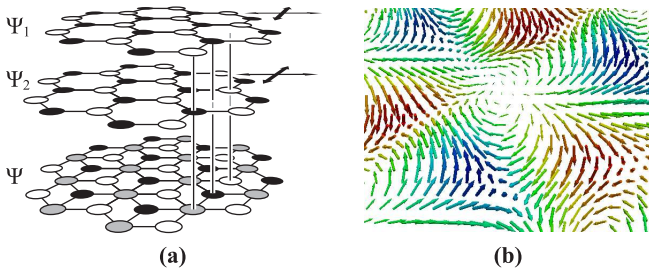


Figure 1: (a) Schematic of two honeycomb vortex-antivortex lattices that combine in the pseudospinor $\Psi = (\Psi_1, \Psi_2)$. The lattices each form due to the interference of three BEC wavepackets initially located at the corners of an equilateral triangle. Arrows represent the ability to control lattice alignment by establishing relative wavepacket phases. (b) Representation using local Bloch vectors scaled by density reveals three textures. In this example, corresponding to the alignment shown in (a), a central spin-2 texture with net zero mass-current (grey circle in (a)) is surrounded by six half-quantum vortices (black and white circles in (a)) distinguished by alternating mass-current circulations.

¹G. Ruben, D. M. Paganin and M. J. Morgan, "Vortex-lattice formation and melting in a nonrotating Bose-Einstein condensate", *Phys. Rev. A* 78, 013631 (2008)

²G. Ruben, M. J. Morgan and D. M. Paganin, "Texture control in a pseudospin Bose-Einstein condensate", arXiv:1005.4760.

Bose statistics and classical fields

Przemyslaw Bienias¹, Krzysztof Pawłowski¹, E. Witkowska² M. Gajda²
K. Rzazewski¹

¹*Center for Theoretical Physics, Polish Academy of Sciences, al. Lotnikow 32/46,
02-668 Warsaw, Poland*

²*Institute of Physics Physics, Polish Academy of Sciences, al. Lotnikow 32/46, 02-668
Warsaw, Poland*

Classical fields counterpart of the ideal and weakly interacting Bose gas statistics in a trap will be investigated by performing calculations in the canonical ensemble. There exists the optimal cut-off which allows to match the full probability distribution of the condensate population by its classical counterpart in the ideal gas case. Universal scaling of that cut-off with temperature and dimensionality will be derived.¹ We then, investigated the weakly interacting bosons using the Monte Carlo method. For the first time statistical properties of a one dimensional Bose gas in a trap are obtained with atom-atom interaction accounted for in all orders. Temperature dependence of the statistics of condensate population as well as low order spatial correlation functions are computed.

¹E. Witkowska et al, Phys. Rev. A **79** 033631 (2009).

Time averaged optical traps for the investigation of superfluidity in BEC

S.K. Schnelle, K. Weegink, E.D. van Ooijen, M.J. Davis, N.R. Heckenberg,
H. Rubinsztein-Dunlop.

School of Mathematics and Physics, The University of Queensland, 4072, Queensland

We present the realization of a time averaged optical trap for the use with Bose-Einstein condensates (BEC). The trap uses a two dimensional acousto-optic modulator (AOM) to spatially scan a tightly focused, red-detuned laser beam to create arbitrary two dimensional static or dynamic potentials. The poster presented will detail the technical questions in optical and electronic design of the trap as well as present first measurements of BEC in time averaged traps.¹ We will also present the idea and mean-field simulations of a scheme to measure the critical velocity of BEC utilizing the time averaged trap. For this a line potential with a moving barrier has been created.

To excite the BEC a barrier will be moved through the condensate with different barrier velocities. The barrier will be started inside the condensate which is held in a very homogeneous trap which should give more precise results than measurements done so far. To achieve this higher precision in determining the critical velocity of BEC it is necessary to generate a very smooth, box-like potential which has been created using first thermal and later condensed atoms to map the potential and subsequently adjusting the intensity of the scanned laser beam in an iterative process until the necessary homogeneity has been achieved.

¹S.K. Schnelle *et. al.*, "Versatile two-dimensional potentials for ultra-cold atoms." Opt. Express 16(3), 1405.

Rotating Bose-Einstein Condensates in Time-Averaged Adiabatic Potentials

B. E. Sherlock, M. Gildemeister, E. Nugent, E. Owen, B. T. Sheard, C. J. Foot,

Clarendon Laboratory, University of Oxford, Parks Road, Oxford, OX1 3PU, U.K.

Rotation of trapped Bose-condensed atomic gases provides an opportunity to study a range of many-body phenomena that are analogous to those in Condensed Matter systems. The nature of superfluidity in two-dimensional systems, the effects of barriers on the decay of persistent currents and the behaviour of a condensate when the imposed rotation rate approaches the limiting value all represent stimulating areas for investigation.

We present the current status and outlook for our experimental approach to create smooth, versatile trapping potentials, within which the behaviour of a Bose-Einstein condensate of ^{87}Rb atoms under varying degrees of rotation can be observed. We employ the first experimental realisation¹ of a Time-Averaged Adiabatic Potential² (TAAP) to confine and manipulate condensates. In our implementation, the TAAP is formed by applying a time-averaging field to the radio frequency (RF) dressed energy levels of a bare quadrupole trap, the resulting potential possessing both harmonic and quartic terms. The design of the magnetic trap affords us 3-axis control over the orientation and polarisation of both dressing and time-averaging fields, and thus the ability to move smoothly between a double well, ring and shell potentials. The vectorial nature of the coupling between atoms and the dressing RF can be exploited to instigate rotation or raise stationary barriers around the potential which change the local speed of sound.

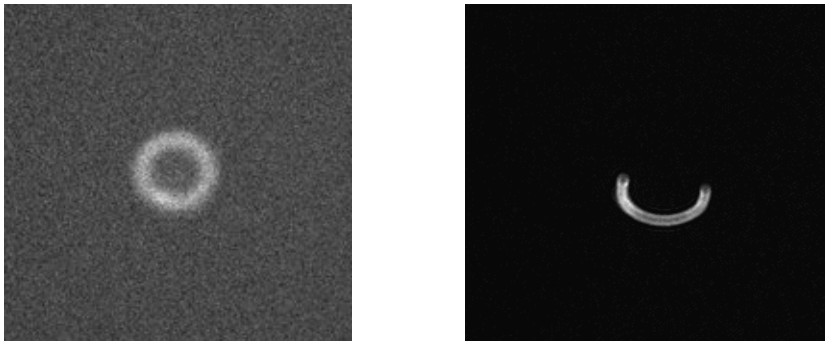


Figure 2: *Images of ultra-cold atoms trapped in the ring (left) and shell (right) potentials.*

¹M. Gildemeister, E. Nugent, B. E. Sherlock, B. T. Sheard, M. Kubasik and C. J. Foot. Trapping ultracold atoms in a time-averaged adiabatic potential. *Phys. Rev. A.*, 81(3):031402, Mar 2010.

²I. Lesanovsky and W. von Klitzing. Time-averaged adiabatic potentials: Versatile matter-wave guides and atom traps. *Phys. Rev. Lett.*, 99(8):083001, Aug 2007.

All-Optical Rb BEC

D. Sigle L. Humbert J.S. Butcher K. Weegink E.D. van Ooijen N.R. Heckenberg
H. Rubinsztein-Dunlop

*School of Physical Sciences, The University of Queensland, Brisbane QLD 4072,
Australia*

We report on our All-Optical Rb⁸⁷ Bose-Einstein condensate experiment which is currently being built. We implement a single beam dipole trap with a 20 W fibre laser at a wavelength of 1064 nm, where the focus has a beam waist of 31 μm . The dipole trap is loaded from a conventional Magneto-optical trap (MOT) with an initial temperature of 220 μK . Molasses cooling is used to optimize the transfer from the MOT to the dipole trap and we achieve temperatures of 50 μK just before transfer. Absorption imaging and fluorescence imaging are implemented which we use to observe loading of the dipole trap from the MOT. We estimate the lifetime of the atoms in the dipole trap to be 6 s. Currently, we are working on optimizing the conditions for optimal evaporative cooling to achieve the transition to BEC. This involves ramping the laser power down from a maximum of 15 W where the laser intensity is controlled via an acousto-optical modulator.

In our setup, a scanning trap will be implemented to trap the BEC in time averaged potentials. We are also investigating the possibility of trapping and cooling Rb⁸⁵ atoms using this setup and to use Feshbach resonances to enhance the evaporation process by increasing the elastic scattering rate and minimize the 3-body losses.

Josephson oscillations of heat - collective excitations of few-mode Bose-Hubbard systems

M.P. Strzys, J.R. Anglin

OPTIMAS Research Center and Fachbereich Physik, Technische Universität Kaiserslautern, D-67653 Kaiserslautern, Germany

The interest in rich phenomena connected to mesoscopic quantum systems is steadily growing over the last years. Such models yield the possibility of investigating the foundations of quantum statistics and connect different branches of research. Because of their theoretical feasibility and their experimental accessibility especially few-mode Bose-Hubbard systems may help to close the gap between microscopic and macroscopic theories.

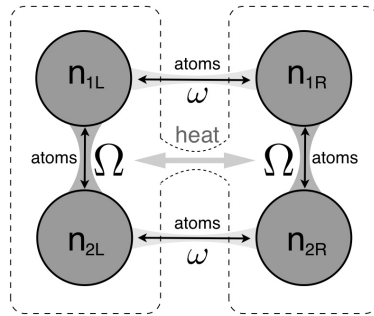


Figure 1: *Four-mode Bose-Hubbard system as model for thermal contact.*

A four-mode Bose-Hubbard model with two highly differing tunneling rates may e.g. be considered as a model for two quantum systems in thermal contact (see Fig. 1). In addition to coherent particle exchange a novel slow second Josephson mode, which is not predicted by linear Bogoliubov theory, can be identified by a series of Holstein-Primakoff transformations¹. This energy exchange mode can be interpreted as heat exchange between the subsystems, is in close analogy to second sound in liquid helium, and may thus shed light on the emergence of thermodynamics in mesoscopic systems.

¹M. P. Strzys, J. R. Anglin, Phys. Rev. A **81**, 043616 (2010)

Formation of vortex superlattice and Bloch domains in a rapidly-quenched and fast-rotating antiferromagnetic spinor Bose-Einstein condensate

S.-W. Su¹, I.-G. Liu², C.-H. Hsueh², Y.-C. Tsai³, T.-L. Horng⁴, S.-C. Gou²

¹*Department of Physics, National Tsing Hua University, Hsin Chu, Taiwan*

²*Department of Physics, National Chang Hua University of Education, Chang Hua, Taiwan*

³*Department of Photonics, Feng Chia University, Taichung, Taiwan*

⁴*Department of Applied Mathematics, Feng Chia University, Taichung, Taiwan*

By solving the stochastic projected Gross-Pitaevskii equation, we investigate the dynamics of an $F = 1$ spinor Bose-Einstein condensate of ^{23}Na during the rotating evaporative cooling. We find that, during the quench, the condensates described by the order parameter $\Psi = (\Psi_1, \Psi_0, \Psi_{-1})$ grow up but in the meantime, quantized vortices nucleate in all three components of the spinor BEC. When the rotating cloud reaches equilibrium at very low temperatures, vortices of each component would closely bind up in pairs and then arrange themselves into some particular spatial structures rather than the conventional triangular Abrikosov lattice. Considering each tightly bound vortex pair as a single entity, and connecting the center-of-mass locations of these pairs, we then find that the vortex pairs in each Ψ_i form a square lattice as a response to the external rotation, when $|\Psi_1|^2 = |\Psi_0|^2 = |\Psi_{-1}|^2$. Furthermore, by stacking up lattices for all spin components, we observe that all three kinds of vortices are paired up to form three interwoven square lattices. Consequently, the overall structure can be regarded as a square superlattice, namely, a lattice with basis, which is made up of six vortices, two for each component. Additionally, the corresponding local spin textures of the spinor BEC are studied. Our numerical calculations indicate that the spin textures, whose projection on the plane perpendicular to the rotating axis forms domains of staggered magnetic moments, can always be decomposed of spin spirals of the Bloch type of domain walls along two orthogonal directions on the rotating plane.

Quantum control of an interacting Bose-Einstein condensate

S. S. Szigeti^{1,2}, M. R. Hush^{1,2}, A. R. R. Carvalho^{1,2} J. J. Hope^{1,2}

¹*Department of Quantum Science, The Australian National University, Australian Capital Territory 0200, Australia*

²*Australian Centre for Quantum-Atom Optics, The Australian National University, Australian Capital Territory 0200, Australia*

The atom laser is the most coherent source for atom optical experiments^{1,2}. However, the applicability of the atom laser as a tool for fundamental research is limited by noise that broadens the linewidth. This noise is due, in part, to instability in the spatial mode of the Bose-Einstein condensate (BEC) from which the atom laser beam is outcoupled. Excitations of the BEC spatial mode exist under general preparation conditions³, and are generated when the atom laser is continuously pumped^{4,5}. One promising solution to this difficulty is to drive the BEC towards a stable spatial mode via the use of measurement feedback control. A control scheme based on a measurement of position has been shown to successfully cool a single atom in a harmonic trap close to the ground state from any initial state⁶. However, although this control scheme can be engineered by placing the atom in a cavity⁷, it is unclear whether it could be generalised to a many-atom BEC.

In this paper we consider a feedback control scheme based upon dispersive imaging, a technique that has already been implemented in multiple BEC laboratories. A stochastic master equation (SME) for the system is derived from a general Hamiltonian based upon system-bath coupling. In a previous paper⁸, numerical solutions for this SME were presented in the limit of a single atom. It was shown that the final steady state energy of the atom is dependent upon the measurement and feedback strengths and the ratio of photon and atomic kinetic energies. Building upon this work, we consider this SME under the Hartree approximation, which is the assumption that the quantum state is a state of fixed total number. This was used in preference to the usual mean-field approximation, as it more appropriately models a BEC under a continuous number-like measurement. We present numerical simulations (generated using the software package `xpdeint`⁹) which indicate that a BEC can be effectively cooled to a steady-state energy, close to the ground state energy, irrespective of the size of the condensate's nonlinearity.

¹M.-O. Mewes, M. R. Andrews, D. M. Kurn, D. S. Durfee, C. G. Townsend and W. Ketterle, *Phys. Rev. Lett.* **78**, 582 (1997).

²P. Bouyer and M. A. Kasevich, *Phys. Rev. A* **56**, R1083 (1997).

³P. D. Drummond and J. F. Corney, *Phys. Rev. A* **60**, R2661 (1999).

⁴S. A. Haine, A. J. Ferric, J. D. Close and J. J. Hope, *Phys. Rev. A* **69**, 013605 (2004).

⁵M. T. Johnsson, S. A. Haine and J. J. Hope, *Phys. Rev. A* **72**, 053603 (2005).

⁶S. D. Wilson, A. R. R. Carvalho, J. J. Hope and M. R. James, *Phys. Rev. A* **76**, 013610 (2007).

⁷A. C. Doherty and K. Jacobs, *Phys. Rev. A* **60**, 2700 (1999).

⁸S. S. Szigeti, M. R. Hush, A. R. R. Carvalho and J. J. Hope, *Phys. Rev. A* **80**, 013614 (2009).

⁹G. Collecute, P. D. Drummond and J. J. Hope, *eXtensible Multi-dimensional Simulator*, documentation and source available from <http://www.xmms.org>.

Kelvin-Roton Instabilities of Vortex States in BEC with Finite-Range Interactions

M. Takahashi¹, T. Mizushima², K. Machida²

¹*Department of Physics, University of Tokyo, Hongo 7-3-1, Bunkyo-ku, Tokyo 113-0033, Japan*

²*Department of Physics, Okayama University, Okayama 700-8530, Japan*

Many interesting phenomena have been studied in a cold atom physics field. One of recently investigated topics is dipolar Bose-Einstein condensate (BEC) systems. After the realization of the BEC with ⁵²Cr atoms, which have larger magnetic moments compared to alkali atoms, many theoretical and experimental investigations have been done for the system. In such system, the dipole-dipole interaction, which is long-range and anisotropic interaction, plays an important role and gives nontrivial ground state and excitation properties. Heteronuclear polar molecules are thought also a good candidate for such system. On the other hand, Henkel *et al.*¹ predicts that an isotropic but finite-range interaction is realizable in the BEC of Rydberg atoms, where the roton-type instability is proposed.

Motivated by such research movement on the BEC field, we consider isotropic finite-range interaction system with a vortex, since finite-range interactions fundamentally change the properties of condensate and the vortex states give additional intriguing phenomena. In addition to bulk roton-type excitations, we found kelvons, which are oscillating modes of vortex lines, and ripples, which are surface fluctuated modes. It is also demonstrated that those instabilities occur before the bulk roton-type instabilities. We solve Gross-Pitaevskii and Bogoliubov-de Gennes equations to take into account of excitation modes.

Our study gives fundamental understanding of the BEC with finite-range interactions, which has variety of excitations extended to the past study of the contact interactions.

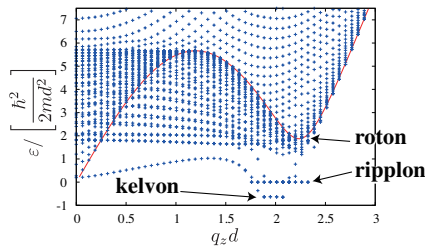


Figure : Excitation spectra with roton-type, kelvon, ripplon instabilities (cross). Solid line shows analytical excitation spectrum in uniform system. Unit length d is coherence length, and m is mass of an atom.

¹N. Henkel, R. Nath, and T. Pohl, Phys. Rev. Lett. **104**, 195302 (2010).

Determination of Scattering Length Using Phase Separation Dynamics near Feshbach Resonance

S. Tojo, Y. Taguchi, Y. Masuyama, and T. Hirano

Department of Physics, Gakushuin University, Tokyo, Japan

We have demonstrated a novel determination of an interspecies s -wave scattering length using phase separations in a spin mixture of a binary Bose-Einstein condensate (BEC) as a diagnostic technique. Spectroscopic techniques such as Ramsey fringe is widely used for precise determination of the scattering length¹. However, it can be applied for only spectroscopic transition between corresponding states and energy shift due to atom density is not negligible for quantum degenerate gases. A binary BEC exhibits phase separation or overlapping under evolution time. The dynamics strongly depends on the scattering length. Feshbach resonance which changes scattering length can control miscibility of binary BEC in different isotopes². A binary ^{87}Rb BEC in mixed hyperfine states in the vicinity of Feshbach resonance was observed at 9.10 G³. We have studied the dynamics of ^{87}Rb binary BEC between $|1, 1\rangle$ and $|2, -1\rangle$ near Feshbach resonance in an optical trap in both experimentally and theoretically. We obtained the difference of the interspecies scattering length ($\Delta a = a_{\text{eff}} - a_{\text{bg}}$; a_{eff} and a_{bg} are effective and background scattering lengths) from diagnostic comparison of density distribution between experimental and theoretical results as shown Fig.1.

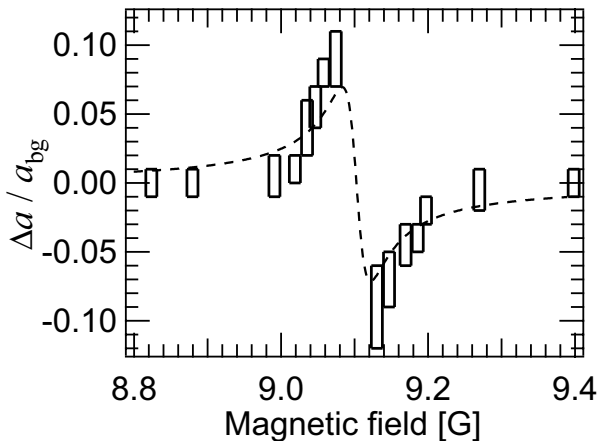


Figure 1: Interspecies scattering length for a magnetic field around the Feshbach resonance. The dashed line is estimated from two body loss rate.

¹D. M. Harber, H. J. Lewandowski, J. M. McGuirk, and E. A. Cornell, Phys. Rev. Lett. **66**, 053616 (2002).

²S. B. Papp, J. M. Pino, and C. E. Wieman, Phys. Rev. Lett. **101**, 040402 (2008).

³M. Erhard *et al.*, Phys. Rev. A **69**, 032705 (2004); A. Widera *et al.*, Phys. Rev. Lett. **92**, 160406 (2004).

Direct Measurement of the Third Order Correlation Function of a Bose-Einstein Condensate

S.S. Hodgman, R.G. Dall, A.G. Manning, M.T. Johnsson, K.G.H. Baldwin,
A.G. Truscott

*Research School of Physics and Engineering, Australian National University,
Canberra, ACT, Australia*

Fundamental to the description of a Bose-Einstein condensate (BEC) is its degree of coherence. From a theoretical point of view a condensate is a macroscopic wavefunction that is characterized by long range order and coherent to all orders. Experimentally, however, higher order correlation functions are difficult to measure, and thus to date only first ¹ and second order ² coherence have been demonstrated for a BEC. We use the unique single atom detection capabilities of a metastable helium (He*) condensate together with a novel experimental procedure ³ to directly measure the third order correlation function for a He* BEC. Above condensation, where the atom cloud is characterised by independent thermal sources, we observe the theoretically predicted factor of three increase (within experimental error) in the amplitude of $g_3(0,0)$ relative to $g_2(0)$, Fig.1. On condensate formation, however, $g_3(\tau_1, \tau_2) = 1$ for all values of τ_1 and τ_2 , thus demonstrating the third order coherence of a BEC.

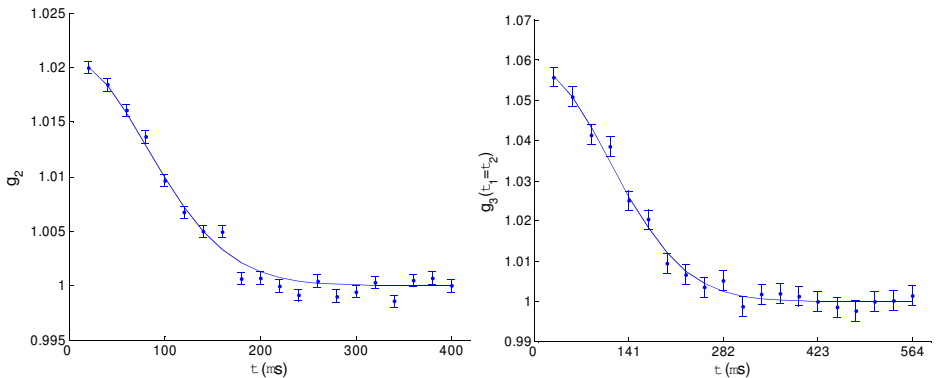


Figure 1: Measured $g_3(\tau, \tau)$ relative to $g_2(\tau)$ above condensation, showing the predicted factor of three enhancement of the bunching amplitude.

¹M.R. Andrews *et al.*, Science **275**, 637 (1997).

²M. Schellekens, R. Hoppeler, A. Perrin, J. V. Gomes, D. Boiron, A. Aspect, and C. I. Westbrook, Science **310**, 648 (2005).

³A.G. Manning, S.S. Hodgman, R.G. Dall, M.T. Johnsson and A.G. Truscott, Submitted to Optics Express (2010).

Time-resolved density correlations as probe of squeezing in toroidal Bose-Einstein condensates

Michael Uhlmann

University of British Columbia, Vancouver, British Columbia, Canada

Toroidal Bose-Einstein condensates offer various opportunities for the study of dynamical quantum effects in nontrivial trap geometries. The confinement potential is usually (almost) isotropic such that the trap is homogeneous with periodic boundary conditions in the azimuthal direction. In the radial direction, however, the trap is generally inhomogeneous.

In this contribution, I study the evolution of mean field and linear quantum fluctuations during an interaction quench from a finite value to zero¹. Initially, the condensate shall be in a quasi-two-dimensional regime with repulsive interaction strength, which is then tuned to zero, i.e., the atoms become non-interacting. Adiabaticity will be violated for sufficiently rapid changes; the system will not stay in its ground state. In view of the isotropy of the trap, any classical mean-field excitations can only be in the radial direction, e.g., radial breathing oscillations, whereas the linear quantum fluctuations are only subject to angular momentum conservation, i.e., quasi-particle excitations must occur in pairs with azimuthal wavenumbers $\pm n$. Thus, azimuthal density correlations, where the radial dependence has been integrated out, would yield a signature of the linear (quantum) fluctuations void of any background motion.

The Fourier spectrum of the azimuthal density correlations is calculated to show temporal oscillations. These temporal oscillations can be directly attributed to the mixing of positive and negative frequencies during the non-adiabatic evolution, i.e., the squeezing of (quasi-)particles out of the condensate. As coherent quasi-particle pairs with wavenumbers $\pm n$ are created, one of the particles must circle the torus clockwise and one must go counter-clockwise. The oscillations could thus be interpreted through co-incidence of the two (coherent) particles: The Fourier component of the correlation function will have a minimum if the two particles are at the same place and a maximum if they are farthest apart. A time-resolved measurement of the azimuthal equal-time density correlation function would thus yield a unique signature of quasi-particle squeezing, i.e., the mixing of positive and negative frequency modes during non-adiabatic evolution, in isotropic toroidal Bose-Einstein condensates. Since the time-dependence of the equal-time correlation is directly related to coherence of the squeezed quasi-particles, a clear discrimination to initially present (incoherent) quasi-particles would also be possible.

¹M. Uhlmann, arXiv:1005.2645

Thermodynamics of quasi-2D boson gases and a BCS-BEC model of high- T_c superconductivity in layered cuprates

C. Villarreal¹, M. de Llano², M. Lomnitz³

¹*Instituto de Física, Universidad Nacional Autónoma de México, Ciudad Universitaria, 04510 México, DF, Mexico*

²*Instituto de Investigaciones en Materiales, Universidad Nacional Autónoma de México Apdo.Postal 70-360, 04510 México, DF, Mexico*

³*Facultad de Ciencias, Universidad Nacional Autónoma de México, Ciudad Universitaria, 04510 México, DF, Mexico*

We study the thermodynamics of a quasi-2D Bose-Einstein gas with a linear energy-momentum dispersion relation $\varepsilon = c_1 p$ constrained within a thin region of finite width δ . We calculate the dependence on δ of relevant thermodynamic quantities such as particle number density, internal energy, free energy, entropy, and specific heat. In particular, for a given particle density n the BEC condensation temperature $k_B T_c = \hbar c_1 (12\delta n/\pi)^{1/2}$.

We use the derived results to construct a model of high- T_c superconductivity in copper oxides with a periodic layered atomic structure within a BCS-BEC formalism with linearly-dispersive s- and d-wave Cooper pairs moving in quasi-2D finite-width layers about the CuO_2 planes. The fact that the BCS interaction yields a linear dispersion relation for small (center of mass) momentum Cooper pairs was first noticed by Schrieffer¹. By evaluating the particle density in terms of the (zero-temperature) in-plane magnetic penetration depth λ_{ab} for particles subject to linear dispersion, we obtain:

$$T_c = \frac{\hbar c}{2\pi k_B e} \sqrt{\frac{3\delta}{2\hbar\omega_D}} \frac{\Delta_0}{\lambda_{ab}} \equiv \frac{\Lambda_T}{\lambda_{ab}}, \quad (1)$$

where Δ_0 is the zero-temperature energy-gap of the BCS formalism, and ω_D the Debye frequency. This formula involves no free parameters and reasonably reproduces empirical values of superconducting T_c s for different layered including *YBCO* with different dopings, from the BEC to the BCS regime, and other compounds like *LSCO*, *BSCCO* and *TBCCO*. In concurrence with Ginzburg-Landau formalism, formula (1) also yields a fair description of the T_c dependence of lower critical magnetic field in highly underdoped *YBCO*:

$$H_{c1}(0) = \frac{\Phi_0}{4\pi\xi^{0.35}} [1 + (\xi/\lambda_{ab})^{0.35}] \frac{1}{\lambda_{ab}^{1.65}} \simeq \frac{\Phi_0}{4\pi\xi^{0.35}} \left[\frac{T_c}{\Lambda_T} \right]^{1.65}, \quad (2)$$

where Φ_0 is the magnetic flux quantum, and ξ is Ginzburg-Landau coherence length. By introducing physical parametrs corresponding to *YBCO* with different dopings, we get $H_{c1}(0) = (0.143 - 0.259) T_c^{1.65 \pm 0.01}$ Oe, in accordance with experimental findings.

¹J.R. Schrieffer, *Theory of Superconductivity* (W.A. Benjamin, Reading, MA, 1964)

Modeling the collision of two ultra-cold clouds of bosons

A.C.J. Wade, P.B. Blakie

Jack Dodd Centre for Quantum Technology, Department of Physics, University of Otago, Dunedin, New Zealand.

Experiments with ultra-cold gases routinely investigate dynamical processes of mesoscopic systems which are far from equilibrium and have complex geometry. Such regimes are well understood for low temperature Bose condensed gases, where the Gross-Pitaevskii equation has proven to provide a comprehensive description. However, very little work has been performed at higher temperatures, except near equilibrium. Here we are motivated to develop techniques for simulating the thermal cloud dynamics experimentally reported by Kjaergaard and coworkers¹². In that work, ultra-cold clouds of bosons were collided at velocities where p -wave² and d -wave¹ scattering became important.

In this work we model those experiments using the quantum Boltzmann equation,

$$\left(\frac{\partial}{\partial t} + \frac{\mathbf{p}}{m} \cdot \nabla_{\mathbf{r}} - \nabla_{\mathbf{r}} U(\mathbf{r}, t) \cdot \nabla_{\mathbf{p}} \right) f(\mathbf{r}, \mathbf{p}, t) = \int \frac{d^3 p_2}{h^3} \int d\Omega \left| \frac{d\sigma}{d\Omega} \right| \frac{|\mathbf{p}_2 - \mathbf{p}|}{m} [(1 + f)(1 + f_2)f_3f_4 - ff_2(1 + f_3)(1 + f_4)],$$

where \mathbf{p} and \mathbf{r} are the phase-space coordinates, $f(\mathbf{r}, \mathbf{p}, t)$ is the distribution function and $U(\mathbf{r}, t)$ is the external potential. The details of the scattering are built into a differential cross-section, $\left| \frac{d\sigma}{d\Omega} \right|$, and the bosonic nature of the atoms is accounted for by the Bose enhancement terms, $1 + f_i$.

We have solved the Boltzmann equation using a test particle method³, which is capable of simulating boltzons, bosons, and fermions in complex geometries and far from equilibrium. We present the results of our simulations of collisions of ultra-cold bosons, finding good agreement with experimental data.

¹N. R. Thomas, N. Kjaergaard, P. S. Julienne, and A. C. Wilson, "Imaging of s and d Partial-Wave Interference in Quantum Scattering of Identical Bosonic Atoms", *Phys. Rev. Lett.* **93** (2004), no. 17, 173201

²A. S. Mellish, N. Kjaergaard, P. S. Julienne, and A. C. Wilson, "Quantum scattering of distinguishable bosons using an ultracold-atom collider", *Phys. Rev. A* **75** (2007), no. 2, 020701

³(e.g. see B. Jackson and E. Zaremba, "Modeling Bose-Einstein condensed gases at finite temperatures with N-body simulations", *Phys. Rev. A* **66** (2002), no. 3, 033606)

Anomalous Tunneling of Spin Wave Excitations in a Spin-1 Spinor Bose-Einstein Condensate

S. Watabe^{1,2}, Y. Kato³, Y. Ohashi^{1,2}

¹*Keio University, Hiyoshi, Yokohama, Japan*

²*CREST(JST), Honcho, Saitama, Japan*

³*The University of Tokyo, Komaba, Tokyo, Japan*

We theoretically discuss tunneling properties of collective spin excitations in an $S = 1$ spinor Bose-Einstein condensate, extending our earlier work¹. Within the mean-field theory, we examine the transmission probability of a transverse spin wave mode through a barrier potential in the case when there exists finite supercurrent of the magnetic sublevel 1. When the momentum q_{spin} of the magnetic sublevel 0, whose wavefunction is associated with the transverse spin wave mode, coincides with that of the supercurrent q_{current} , we show that the perfect transmission of the spin wave mode is realized. This is quite different from the so-called anomalous tunneling phenomenon of Bogoliubov excitations², where the perfect transmission of the Bogoliubov mode always occurs in the long wavelength limit $q = 0$, unless the system is in the critical current state³. Indeed, in the long wavelength limit, the spin wave mode is found to show the perfect *reflection*. We clarify that this q -dependent anomalous tunneling (perfect transmission) behavior of the spin wave excitations is deeply related to the similarity between the wavefunction of the magnetic sublevel 0 and the condensate wavefunction near $q_{\text{spin}} = q_{\text{current}}$.

¹S. Watabe and Y. Kato, *Journal of Low Temp. Phys.* **158**, 23 (2010).

²Yu. Kagan, D. L. Kovrizhin, and L. A. Maksimov, *Phys. Rev. Lett.* **90**, 130402 (2003).

³I. Danshita, N. Yokoshi, and S. Kurihara, *New J. Phys.* **8**, 44 (2006).

The small-scale behavior of turbulent atomic Bose-Einstein Condensates

A. C. White¹, M. J. Davis¹, C. J. Foster¹, C. F. Barenghi²

¹*ARC Centre of Excellence for Quantum Atom Optics, School of Mathematics and Physics, The University of Queensland, Brisbane 4072 QLD, Australia*

²*School of Mathematics and Statistics, Newcastle University, Newcastle upon Tyne, NE1 7RU, England, UK*

Despite its widespread prevalence in nature, understanding turbulence remains one of the longest unsolved problems in classical physics. Exploring turbulence in quantum systems is an innovative way to shed light on this fundamental physics problem. In classical turbulence vorticity is continuous and eddies can be of any size and strength. In superfluids such as Bose-Einstein condensates, vortices are topological defects with quantized circulation, making turbulence in these quantum systems easier to study than classical turbulence. While fundamentally different mechanisms determine the dynamics of quantum and classical turbulence, remarkable similarities between classical and quantum turbulence exist. One striking similarity is the same Kolmogorov energy spectrum arising in continuously excited turbulence¹.

Here we investigate the mechanism dominating the decay of turbulent atomic Bose-Einstein Condensates at scales smaller than the average distance between vortices in the vortex tangle and larger than the vortex core diameter. At these small length scales, oscillations of vortex lines known as Kelvin waves, arising from reconnections between vortices in the turbulent tangle are thought to dominate the energy dissipation process². Turbulence is induced in our 3D simulations by two techniques, phase-imprinting vortex rings and lines, or alternatively, initially imposing a random phase on the condensate. The condensate dynamics are modelled for the homogeneous case by evolving the projected Gross-Pitaevskii equation³.

¹J. Maurer and P. Tabeling, "Local investigation of superfluid turbulence", *Europhys. Lett.*, **43** 29 (1998); C. Nore, M. Abid and M. E. Brachet, "Kolmogorov Turbulence in Low-Temperature Superflows", *Phys. Rev. Lett.*, **78** 3896 (1997); T. Araki, M. Tsubota and S. K. Nemirovskii, "Energy Spectrum of Superfluid turbulence with No Normal-Fluid Component", *Phys. Rev. Lett.*, **89** 145301 (2002); M. Kobayashi and M. Tsubota, "Kolmogorov Spectrum of Superfluid Turbulence: Numerical Analysis of the Gross-Pitaevskii Equation with a Small-Scale Dissipation", *Phys. Rev. Lett.*, **94** 065302 (2005).

²D. Kivotides, J. C. Vassilicos, D. C. Samuels and C. F. Barenghi, "Kelvin Waves Cascade in Superfluid Turbulence", *Phys. Rev. Lett.*, **86** 3080 (2001).

³P. B. Blakie, A. S. Bradley, M. J. Davis, R. J. Ballagh and C. W. Gardiner, "Dynamics and statistical mechanics of ultra-cold Bose gases using c-field techniques", *Advances in Physics*, **57** 363 (2008); N. P. Proukakis and B. Jackson, "Finite-temperature models of Bose-Einstein condensation", *J. Phys. B: At. Mol. Opt. Phys.*, **41** 203002 (2008).

Controlling one-dimensional spin dynamics with state-dependent potentials

P. Wicke, S. Whitlock, N. J. van Druten

Van der Waals-Zeeman Institute, University of Amsterdam, The Netherlands

Reducing the dimensionality of a system has dramatic consequences, often leading to remarkable new physics. In this regard, one-dimensional quantum gases offer unique opportunities to address important open questions in quantum many-body physics through exact comparisons to theory and precise experimental control of all relevant parameters. Exhibiting even richer quantum effects than its single component counterpart, the two-component one-dimensional Bose gas captures the complex interplay between internal (spin) and external (motion) degrees of freedom, relevant to our understanding of phenomena such as spin waves, spin-charge separation, superfluidity and magnetism.

We report the observation and experimental control of spin dynamics in a one-dimensional two-component degenerate Bose gas on an atom chip. The spin dynamics are initiated after creating a coherent superposition of the magnetically trapped clock states of ^{87}Rb . Small differences in interatomic interactions drive the spatial separation of spin components. We present a new method to experimentally control interactions in this system by the application of state-dependent radio-frequency (rf) dressed potentials. This enables, for instance, access to the point where spin dynamics are frozen (relevant for cold atom metrology) and to the point of spin-independent interactions where exact quantum many-body solutions are available.

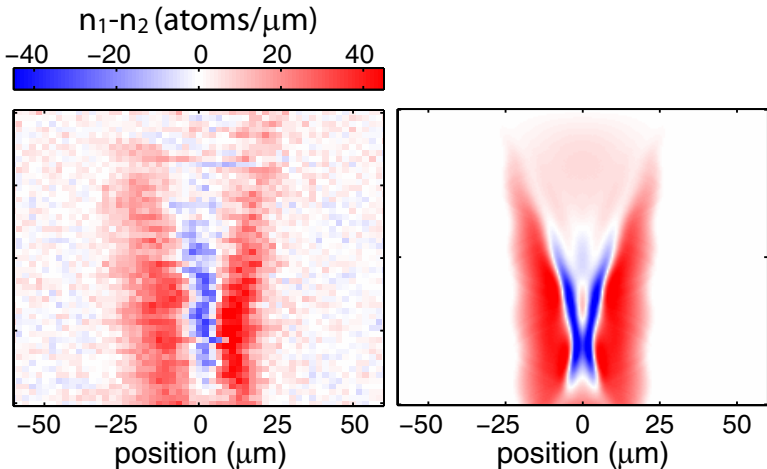


Figure 1: *Measured evolution of spin polarization ($n_1 - n_2$) of a one-dimensional degenerate Bose gas (left). Corresponding numerical Gross-Pitaevskii ($T = 0$) simulation (right).*

Phases of vortex matter in rotating Bose-Einstein condensates

T. M. Wright, M. J. Davis

ARC Centre of Excellence for Quantum-Atom Optics, School of Mathematics and Physics, University of Queensland, Brisbane, Queensland 4072, Australia

The nature of the thermal melting transition of two-dimensional crystals is a topic significant to many fields of research, ranging from type-II superconductors^{1,2} to liquid crystals³ and lipid membranes⁴. The Halperin-Nelson theory⁵ of 2D melting predicts that the process involves *two* transitions: the long-range positional order of the lattice is lost at a lower temperature than the orientational order, resulting in the appearance of an intermediate *hexatic* phase. However, experiments in superconductor vortex lattices² and liquid-crystal films³ suggest that a further intermediate phase may arise, challenging our theoretical understanding of the nature of melting in two dimensions.

It has been suggested⁶ that the thermal melting of vortex lattices in rotating Bose-Einstein condensates is defect mediated, as in the Halperin-Nelson description. Here we characterize the melting of vortex lattices in rotating Bose condensates using a *classical-field* formalism⁷, which includes the effects of thermal fluctuations of the Bose field nonperturbatively. We consider the changes in the structure of the vortex lattice as the temperature of the system is increased, and quantify the positional and orientational correlations between vortices. We compare the vortex-vortex correlations with those of the Bose field itself, and discuss the nature of vortex matter in the regime between a rigid vortex lattice and an isotropic vortex liquid.

¹G. Blatter *et al.*, Rev. Mod. Phys. **66**, 1125 (1994).

²I. Guillamón *et al.*, Nat. Phys. **5**, 651 (2009).

³C.-F. Chou *et al.*, Science **280**, 1424 (1998).

⁴S. L. Veatch *et al.*, Proc. Natl. Acad. Sci. U.S.A. **45**, 17650 (2007).

⁵B. I. Halperin and D. R. Nelson Phys. Rev. Lett. **41**, 121 (1978).

⁶S. A. Gifford and G. Baym, Phys. Rev. A **70**, 033602 (2004); **78**, 043607 (2008).

⁷P. B. Blakie *et al.*, Adv. Phys. **57** 363 (2008).

Towards a Dual-species BEC of Noble and Alkali Gases on an Atom Chip

Wu Rugway¹, Brenton Hall², Lesa Byron¹, Robert Dall¹, and Andrew Truscott¹

¹*Research School of Physics & Engineering, Australian National University*

²*Atom Optics & Ultrafast Spectroscopy, Swinburne University*

The ultimate goal of our work is the production of a dual species Bose-Einstein condensate (BEC) of metastable helium ($^4\text{He}^*$) and rubidium 87 (^{87}Rb). To date we have loaded these species simultaneously into a magneto-optical trap (MOT), and measured the collisional loss rates due to Penning ionisation. Loss rates have also been investigated for the dual species in a magnetic trap, where the spin polarisation occurring in this trap leads to ionisation being suppressed by a factor of at least 100^1 (shown in figure 1). This is encouraging for our objective to trap these species simultaneously on an atom chip² for the production of a dual species BEC. We have been able to load up to 5×10^6 He^* atoms into a z-wire magnetic trap on an atom chip³, with the initial aim to form a He^* BEC.

The unique features of $^4\text{He}^*$ allow atom clouds trapped on a chip to be used for surface probing or investigating quantum reflection. Sympathetic cooling could be achieved with the addition of ^{87}Rb , leading to a dual species condensate ideal for the study of interspecies collisions. It may be possible to find Feshbach resonances between $^4\text{He}^*$ and ^{87}Rb , and even produce heteronuclear diatomic molecules.

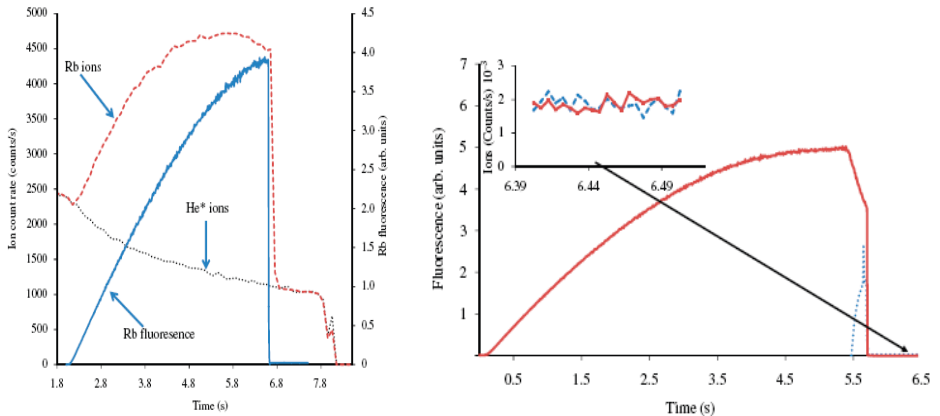


Figure 1: Ion production rates measured - Left: unpolarized case. Right: polarized.

¹L. Byron et. al., Suppression of Penning ionization in a spin-polarized mixture of rubidium and He^* , *New J. Phys.* **12**, 013004 (2010)

²S. Aubin, et al. Trapping Fermionic ^{40}K and Bosonic ^{87}Rb on a Chip *J. Low Temp. Phys.* **140**, 377 (2005)

³Ron Folman et. al., Microscopic atom optics: from wires to an atom chip, *Adv. in At. Mol. Opt. Physics* **48**, 263 (2002)

Large Production of Bose-Einstein Condensate in a Tilted Dipole Trap

B. Yan^{1,2}, M. F. Han^{1,2}, J. Y. Zhang^{1,2}, Z. D. Du^{1,2}, S. Chen^{1,2}, J. W. Pan^{1,2}

¹*Hefei National Laboratory for Physical Sciences at Microscale and Department of Modern Physics, University of Science and Technology of China, Hefei, Anhui, 230026, P. R. China*

²*Center for Quantum Engineering, University of Science and Technology; No. 99, Xiupu road, Pudong new district, Shanghai, 201315, P. R. China*

Quantum simulation based on ultracold atoms provides a new way to explore, especially some complex systems, such as the condensed matter physics. To reach such goals, Bose-Einstein condensate (BEC) is the key element and basis. Because the dipole trap can trap atoms with different Zeeman states, has much tight confinement and efficient evaporative cooling. It can be used to form BEC quickly and provides a nice platform to control the atom interaction through the Feshbach resonance, simulating many body physics¹ In this paper, a simple scheme of producing a relative large BEC in a dipole trap is described. Only two simple steps are added to a regular dipole trap scheme: the temporal dark MOT and tilting the dipole trap. The temporal dark MOT increases the atom intensity, and tilting the dipole trap increases the evaporative cooling efficiency². The measurement of the aspect ratio in different time of flight and the bimodal density distribution prove the producing of a BEC. Our BEC contains 5×10^5 atoms and the transition temperature is about $350nK$. It is a good start towards the quantum simulation.

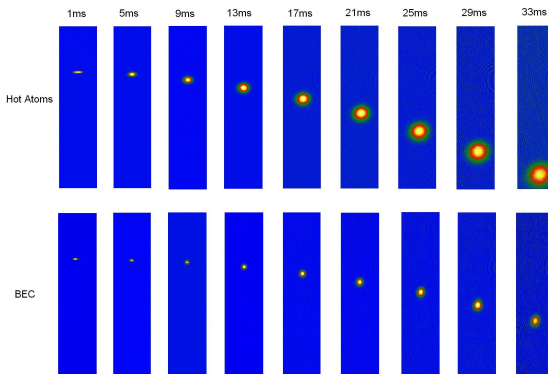


Figure 1: *The images of atoms in different time of flight. The nonisotropic expansion shows the exist of BEC.*

¹R. Grimm, M. Weidemuller, and Y. B. Ovchinnikov, *Advances in Atomic molecular, and Optical Physics*, Vol. 42, 95 (2000).

²C. L. Hung, X. B. Zhang, N. Gemelke, and C. Chin, *Physical Review A* 78 (2008).

Manipulation of the quantum state of a Bose-Einstein Condensate using superradiance

Xiaoji Zhou, Fan Yang Xuguang Yue, Wei Xiong, Yueyang Zhai, Xu Xu,
Xuzong Chen

*School of Electronics Engineering and Computer Science, Peking University, Beijing
100871, China*

Superradiance scattering from a Bose-Einstein condensate is studied with a two-frequency pumping beam. Different momentum states of BECs can be obtained through adjusting the parameters of pump laser beams in the sequential superradiance scattering process¹. We found that the distribution of atomic side modes, which reflects the dynamics of sequential scattering directly, and the depletion behavior of the condensate shows obvious sensitivity to the frequency difference between the two pump components. When the frequency difference is tuned to the predicted resonance frequency, an almost diagonal distribution is obtained with a long pulse duration, different from the case of single-frequency pumping where an X-shaped pattern is only observed with short and intense pump pulse. A variant of the X-shaped pattern is obtained with a frequency difference of $8\omega_r$, which compensates the detuning barriers along diagonal directions. The depletion behavior of the condensate also shows sensitivity to the frequency difference, the central of which shows correlation with the onset of mode $(2, 0)$. Our results present the ability to control the sequential dynamics of BEC superradiance on a large time scale by composing the pump beam.

The dependence of the scattering process on the relative initial phase between the two frequency component is also studied². This dependence, which is not predicted before, is related to two matter gratings, one formed by the condensate at rest plus the side mode with positive momentum, the other by the condensate at rest plus the side mode with negative momentum, both of which scatter end-fire modes photons, and in the end affects the atom-scattering process. The relative optical phase is found to be imprinted on matter wave gratings and can enhance or annihilate scattering in backward modes.

A more general case is studied theoretically through multi-frequency components pumping along the long axis of an elongated Bose-Einstein condensate³. Through the analysis of the the spatial and time evolution of superradiant scattering, we show that high-order forward mode can be obtained by providing the pumping beam with resonant frequency components, which is resulting from mode competition between the different resonant channels and the local depletion of the spatial distribution in the superradiant Rayleigh scattering. Our result is beneficial to a larger momentum transfer in atom manipulation for the atom interferometry and atomic optics.

¹Fan Yang, Xiaoji Zhou, Juntao Li, Yuankai Chen, Lin Xia, and Xuzong Chen, Phys. Rev. A **78**, 043611 (2008).

²Xiaoji Zhou, Fang Yan, Xuguang Yue, T. Vogt, and Xuzhong Chen, Phys. Rev. A **81**, 013615 (2010).

³Xiaoji Zhou, Jiageng Fu, and Xuzong Chen, Phys. Rev. A **80**, 063608 (2009).